Vegetation and geochemical responses to Holocene rapid climate change in Sierra Nevada (SE Iberia): The Laguna Hondera record

Jose Manuel Mesa-Fernández[1, 2], Gonzalo Jiménez-Moreno[1], Marta Rodrigo-Gámiz[2], Antonio García-Alix[1,2], Francisco J. Jiménez-Espejo[3], Francisca Martínez-Ruiz[2], R. Scott Anderson[4], Jon Camuera[1] and María J. Ramos-Román[1]

[1] Departamento de Estratigrafía y Paleontología, Universidad de Granada (UGR), Avda. Fuente Nueva s/n, 18002, Granada, Spain

[2] Instituto Andaluz de Ciencias de la Tierra (IACT), CSIC-UGR, Avenida de las Palmeras 4, 18100, Armilla, Granada, Spain

[3] Department of Biogeochemistry (JAMSTEC), Yokosuka, Japan.

[4] School of Earth Sciences and Environmental Sustainability, Northern Arizona University, Flagstaff, AZ, USA.

Correspondance to: Jose Manuel Mesa-Fernández (jmesa@iact.ugr-csic.es)

Abstract.

High-altitude peat bogs and lacustrine records are very sensitive to climate changes and atmospheric dust input. Recent studies have shown a close relationship between regional climate aridity and enhanced eolian input to lake sediments. However, changes in regional-scale dust fluxes due to climate variability at short-scales and how alpine environments were impacted by climatic- and human-induced environmental changes are not completely understood.

Here we present a multi-proxy (palynological, geochemical and magnetic susceptibility) lake sediment record of climate variability in the Sierra Nevada (SE Iberian Peninsula) over the Holocene. Magnetic susceptibility and geochemical proxies obtained from the high mountain lake record of Laguna Hondera evidence humid conditions during the Early Holocene, while a trend towards more arid conditions is recognized since ~7000 cal yr BP, with enhanced Saharan eolian dust deposition until Present. This trend towards enhanced arid conditions was modulated by millennial-scale climate variability. Relative humid conditions occurred during the Iberian Roman Humid Period (2600-1450 cal yr BP) and predominantly arid conditions occurred during the Dark Ages and the Medieval Climate Anomaly (1450-650 cal yr BP). The Little Ice Age (650-150 cal yr BP) is characterized in the LH record by an increase in runoff and a minimum in eolian input. In addition, we further suggest that human impact in the area is noticed through the record of *Olea* cultivation, *Pinus* reforestation and Pb pollution during the Industrial Period (150 cal yr BP-Present). Furthermore, we estimated that the correlation between Zr and Ca concentrations stands for Saharan dust input to the Sierra Nevada lake records. These assumptions support that present-day biochemical observations, pointing to eolian input as the main inorganic nutrient source for oligotrophic mountain lakes, are comparable to the past record of eolian supply to these high-altitude lakes.

1. Introduction

The southern Iberian Peninsula has been the location for a number of recent studies detailing past vegetation and former climate of the region (Carrión et al., 2001, 2003, 2007, 2010; Carrión, 2002; Combourieu Nebout et al., 2009; Jiménez-Espejo et al., 2008; Martín-Puertas et al., 2008, 2010; Fletcher et al., 2010;

Nieto-Moreno et al., 2011, 2015; Rodrigo-Gámiz et al., 2011; Moreno et al., 2012 Jiménez-Moreno et al., 2015). Some of these studies have also documented that the western Mediterranean area has been very sensitive to short-term climatic fluctuations throughout the Holocene (e.g., Fletcher and Sánchez-Goñi, 2008; Combourieu Nebout et al., 2009; Fletcher et al., 2010; Jiménez-Moreno et al., 2013). However, a subset of recent studies have attempted to determine how Mediterranean alpine environments have been affected by Holocene climate change through the study of sedimentary records from high elevation wetlands in the Sierra Nevada (Anderson et al., 2011; García-Alix et al., 2012, 2013; Jiménez-Moreno and Anderson, 2012; Jiménez-Moreno et al., 2013; Jiménez-Espejo et al., 2014; Ramos-Román et al., 2016; García-Alix et al., 2017). These alpine lake and bog records show minimal anthropic influence because they are usually elevational higher than major regional Late Holocene human landscape modification. This allows for a potentially clearer climatic signal to be determined from these sites. Even though human impact is less important at high-elevations, the impacts of human activities has also been reconstructed from these Late Holocene sedimentary records (Anderson et al., 2011; García-Alix et al., 2012, 2013; 2017, 2018).

Several studies have highlighted the role of atmospheric mineral dust deposition in marine (Pulido-Villena et al., 2008a) and terrestrial (Morales-Baquero et al., 1999; Ballantyne et al., 2011) ecosystem fertilization through major micronutrients supply. Similar results have been described in the Sierra Nevada alpine lakes, where Saharan dust is especially important in conditioning plankton communities from oligotrophic lakes (Morales-Baquero et al., 2006a, 2006b; Mladenov et al., 2008; Pulido-Villena et al., 2008b; Reche et al., 2009). Although this eolian signal has been occasionally recorded in the sedimentary sequences from the Sierra Nevada lakes (Jimenez-Espejo et al., 2014; García-Alix et al., 2017), the record of inorganic nutrients in Saharan dust input in past lake geochemistry has remained elusive. This study investigates a multiproxy sediment core record from Laguna Hondera (LH), located in the Sierra Nevada range with two main goals: (1) identifying and characterizing climatic variability during the Holocene, focusing on vegetation changes, eolian input and runoff sediments variations; and (2) understanding the Saharan dust influence in past lake sedimentation and geochemistry.

2. Study Area

Sierra Nevada is the highest mountain range in the southern Iberian Peninsula. Bedrock of the high elevations of the Sierra Nevada is mostly composed of metamorphic rocks, principally mica schists (Castillo Martín, 2009). During the late Pleistocene, the Sierra Nevada was one of the southernmost mountains to support alpine glaciers and its last advance was recorded during the Little Ice Age (LIA; Palma et al., 2017; Oliva et al., 2018). Subsequently to the melting of ice at the end of the Last Glacial Maximum, wetlands and small lakes formed in the glacial cirque basins, which occur between 2451 and 3227 masl (Schulte, 2002; Castillo Martín, 2009; Palma et al., 2017). Several alpine wetland and lakes have been studied in this area during the last few years as shown in Figure 1.

2.1. Regional Climate and Vegetation

Mediterranean climate characterises southern Iberia, with a marked seasonal variation between warm and dry summers and cool and humid winters (e.g. Lionello et al., 2006). Overprinting this general climate is the influence of the North Atlantic Oscillation (NAO) (Trigo et al., 2004; Trouet et al., 2009). Southern

Iberia is also characterized by strong altitudinal contrasts, which in turn control the precipitation patterns, with mean annual values ranging from <400 mm yr^{-1} to >1400 mm yr $^{-1}$ in the southeast desert lowlands and the southwest highland, respectively (Jiménez-Moreno et al., 2013 and references therein).

As with most mountainous regions, species and species groupings in the Sierra Nevada are distributed with respect to elevation, depending on the temperature and rainfall gradients (e.g., El Aallali et al., 1998; Valle, 2003). Above 2800 masl the crioromediterranean flora occurs as tundra-like open grassland. The oromediterranean belt (1900-2800 masl) mostly includes dwarf *Juniperus* (juniper), xerophytic shrublands and pasturelands and *Pinus sylvestris* and *P. nigra*. The supramediterranean belt (~1400-1900 masl) is characterized by mixed deciduous and evergreen forest species (i.e., evergreen and deciduous *Quercus*, with *Pinus spp.* and others). Mesomediterranean vegetation (600-1400 masl) includes sclerophyllous shrublands and evergreen *Quercus* woodlands. The natural vegetation has been strongly altered by human activities and cultivation in the last centuries, increasing significantly the abundance of *Olea* (olive), due to cultivation at lower altitudes (Anderson et al., 2011, and references therein), and *Pinus* due to reforestation primarily at higher elevations (Valbuena-Carabaña, 2010).

2.2. Laguna Hondera

Laguna Hondera (hereafter LH; 2899 masl; 37º02.88'N, 3º17.66'W, lake surface: 0.0053 km^2; maximum depth: 0.8 m; Morales-Baquero et al., 1999; Fig. 1) is a small and shallow lake located at the lowest elevation of a set of lakes locally named Cañada de Siete Lagunas, a glacial valley between two of the highest peaks of the mountain range in the Iberian Peninsula: Alcazaba (3366 masl) and Mulhacén (3479 masl). LH has a large catchment area of 1.546 km^2, which is much larger than previously studied sites in the region (Laguna de Río Seco, LdRS, 0.099 km^2; Borreguil de la Caldera, BdlC, 0.62 km^2; Morales-Baquero et al., 1999; Ramos-Román et al., 2016; Fig 1 for locations). The lake was reduced to a little pond in the deepest area of the basin when cored in September 2012, with a maximum depth of only a few centimetres.

LH presently occurs in the crioromediterranean vegetation belt (2800 masl) (El Aallali et al., 1998; Valle et al., 2003). The bedrock in the LH basin consists in Paleozoic and Precambrian mica schist with disthene and staurolite of the lower part of the Caldera Formation (Díaz de Federico et al., 1980).

3. Methods

3.1. Core sampling, lithology and chronology

Six sediment cores were recovered from LH with a Livingstone piston corer in September 2012. LH 12-03 (83 cm) was selected for a multi-proxy study because it was the longest core. Cores were wrapped with tin foil and plastic film and transported to Universidad de Granada, where they were stored at 4ºC.

Core LH 12-03 was split longitudinally and the sediments were described. Magnetic susceptibility was measured every 0.5 cm with a Bartington MS2E meter in SI units (x 10^{-4}) (Fig. 2). The sediment cores were subsampled every 1 cm for several analyses, including pollen and geochemistry.

The age model was built using seven AMS radiocarbon dates from vegetal remains (Table 1; Fig. 2) by means of Clam software (Blaauw, 2010; version 2.2), which used the IntCal13 curve for radiocarbon age calibration (Reimer et al., 2013). A smooth spline approach was chosen (Fig. 2). The sediment accumulation rate (SAR) was calculated with the average rate from the Clam smooth spline output (Fig. 2).

3.2. Pollen

Pollen analysis was performed on 1 cm^3 of sample collected at regular 1 cm interval throughout the first 62 cm of the core. Older sediments (from 62 to 82 cm depth) were barren in pollen, and only one interval at 73 cm could be studied (Fig. 2). Pollen extraction included HCl and HF treatment, sieving, and the addition of Lycopodium spores for calculation of pollen concentration (modified from Faegri and Iversen, 1989). Sieving was done using a 10 µm nylon sieve. The resulting pollen residue was suspended in glycerine and mounted on microscope slides. Slides were analysed at 400x magnification counting a minimum of 300 pollen grains. An overview of pollen taxa with abundances >1% for core LH 12-03 is plotted using the Tilia software (Grimm, 1993) in Figure 3. Terrestrial pollen percentages, including Pinus (see discussion below) were calculated based on the total pollen sum excluding the aquatics and wetland pollen (Cyperaceae, Ranunculaceae and Typha), since they record a more local environmental signal. Percentages for aquatics and wetland pollen plotted in Figure 3 were calculated based on the total pollen sum. The pollen zonation was delimitated visually by a cluster analysis constrained by age of taxa abundance >1% using CONISS software (Grimm, 1987) (Fig. 3). *Olea* was differentiated from others Oleaceae, such as *Phillyrea*, because *Olea* present a thicker endexine and higher size of reticulum in polar vision than *Phillyrea* (Beug, 2004).

3.3. Geochemical analyses

X-ray fluorescence (XRF) Avaatech core scanner®, located at the University of Barcelona, was used to measure light and heavy elements in the LH 12-03 core. An X-ray current of 650 µA, a 10 second count time and 10 kV X-ray voltage was used for measuring light elements, whereas 1700 µA X-ray current, 35 second count time and 30 kV X-ray voltage was used for heavy elements. Sampling interval for these analyses was every 0.5 cm. For our study only three elements (K, Ca and Ti) have been considered with enough counts to be representative.

Inductively coupled plasma-optical emission spectrometry (ICP-OES; Perkin-Elmer optima 8300) was used for major element analysis on discrete samples every 2 cm. Prior to analysis, the samples were dried in an oven and digested with HNO_3 and HF. Blanks and international standards were used for quality control, the analytical accuracy was higher than ± 2.79% and 1.89% for 50 ppm elemental concentrations of Al and Ca, respectively, and better than ± 0.44% for 5 ppm elemental concentrations of K.

Trace element analysis was performed with an inductively coupled plasma mass spectrometry (ICP-MS; Perkin Elmer Sciex Elan 5000). Samples were measured in triplicate through spectrometry using Re and Rh as internal standards. The instrumental error is 2% for elemental concentrations of 50 ppm (Bea, 1996). Both ICP-OES and ICP-MS analyses were performed at the Centre for Scientific Instrumentation (CIC), University of Granada, Spain.

3.4. Mineralogical analyses

Morphological and compositional analyses were performed using scanning electron microscopy (SEM) with an AURIGA model microscope (Carl Zeiss SMT) coupled with energy-dispersive X-ray microanalysis

(EDX) and Electron Backscatter Diffraction (EBSD) mode, also at the CIC (University of Granada, Spain). Mineral grains were analysed to determine provenance, in particular those from eolian origin.

3.5 Statistical Analysis

R-mode principal components analysis (PCA) was run on the geochemical dataset using the PAST software (Hammer et al., 2001). PCA identifies hypothetical variables (components) accounting for as much as possible of the variance in multivariate data (Davis, 1986; Harper, 1999). The elements used in the PCA were standardized by subtracting the mean and dividing by the standard deviation (Davis, 1986). Pb was not included in the PCA analysis due to its anthropogenic origin from mining and industrial pollution during the latest Holocene in this area (García-Alix et al., 2013).

4. Results

4.1. Lithology and magnetic susceptibility

The LH 12-03 sediment core consists primarily of peat in the upper ~60 cm, with mostly sand and clay layers below (Fig. 2). Positive MS peaks coincide with the grey clay intervals between 58 and 72 cm. Peat intervals coincide with relatively low MS values. For example, a minimum in MS occurs at 36-48 cm depth, related with a peaty interval with root remains. Near the bottom of the core, between 76 and 80 cm, a sandy oxidized interval occurs.

4.2. Chronology and sedimentation rate

The age model of LH 12-03 documents that the record spans the last 10800 cal yr BP (Table 1; Fig. 2). Sediment accumulation rates (SAR) were calculated using the average rate from the Clam smooth spline output (Fig. 2). The SAR below ~39 cm is very constant, varying between 0.049 and 0.061 mm yr^{-1}. The SAR increases exponentially to 0.098 mm yr^{-1} at 22 cm, 0.167 mm yr^{-1} at ~9 cm and 0.357 mm yr^{-1} at the core top. Accordingly with the model age and the SAR, resolution of pollen analysis varies between ~40 years per sample in the top of the core and ~120 years per sample in the lower part. The resolution of the geochemical analysis on discrete samples changes between 100 and 400 years per sample, but the geochemical XRF core scanning resolution ranges between 15 and 100 years per sample, providing higher resolution than geochemical data on discrete sample. The MS analyses resolution variates between 15 and 100 years per sample.

4.3. Pollen

Fifty distinct pollen taxa were recognized, but only those with abundance higher than 1% are included in the pollen diagram (Fig. 3). Four pollen zones for the LH 12-03 record are identified, using variation in pollen species plotted in Figure 3 and a cluster analysis run through the CONISS software (Grimm, 1987). Zone LH-1 (core bottom-2600 cal yr BP) is subdivided in two subzones. Subzone LH-1A (bottom-4000 cal yr BP) is defined by the alternation between Arboreal Pollen (AP) and herbs. AP is composed primarily of *Pinus*, but also *Quercus*. During the interval from ~9500 to ~7000 cal yr, BP only two samples were analysed, due to the low preservation of pollen in this interval. Pollen in this period is dominated by an alternation between Asteraceae (3-60%) and *Pinus* (5-60%) (Fig. 3). The highest occurrence of Onagraceae (~10%) is identified in this subzone, and Caryophyllaceae reach high values (~10%) as well. Only minor amounts of graminoids (Poaceae and Cyperaceae) occur during this period.

Between ~7000 to ~4000, *Pinus* pollen variates from 70 % to ~55%, with a minimum (~30%) at 5000 cal yr BP. *Quercus* increase from ~2% to ~10%. The highest percentages of *Betula* (~5%) in the record occurs at this time. Asteraceae pollen decreases (~5-30%), but Poaceae increase from <5% at the opening of the subzone to >25%. Cyperaceae occur in high percentages (15%).

The subzone LH-1B (~ 4000-2600 cal yr BP) is defined primarily by a great increase in Poaceae pollen (to ~60%) (Fig. 3). Other important herbs and shrubs include Asteraceae (5-15%) and Caryophyllaceae (~5%). Other pollen types that increase for the first time in this zone include Ericaceae (~3%), *Artemisia* (~3%) and Ranunculaceae (~2-6%). *Pinus* (~3-25%) and Cyperaceae (0-14%) record a minimum in this zone, and Onagraceae disappear altogether (Fig. 3).

Zone LH-2 (~ 2600-1450 cal yr BP) pollen assemblages show high variability. *Pinus* pollen variates between ~80% to ~3% from the onset to the end of the zone. Aquatic pollen such as Cyperaceae (~15%) increases. On the other hand, an increase in herbs such as Asteraceae (~5-70%) occurs along the zone, Poaceae pollen variates between ~7 and 12%.

Zone LH-3 (~ 1450-150 cal yr BP) is subdivided in two subzones. Subzone 3A (~1450-600 cal yr BP) is characterized by an increase in herbaceous pollen, led by Poaceae (~35% maximum during this zone), Asteraceae (~60% maximum during this zone after ~1000 cal yr BP) and *Artemisia* (~10%), with the resulting decrease in AP. Since this subzone to the Present, *Quercus* pollen is the major component of AP instead of *Pinus*. Cyperaceae also show a decrease, and Ranunculaceae reach ~ 5%. Subzone 3B (~600-150 cal yr BP) documents an increase in *Olea* (~6%), Poaceae (20%), Caryophyllaceae (7%) and *Artemisia* (~2-20%). *Pinus* (~2%) and Asteraceae (~20%) decrease in this period. Aquatic and wetland pollen show a rise (Cyperaceae ~30%, Rannunculaceae ~10%).

Zone LH-4 (~ 150 cal yr BP-present) depicts a further increase in *Olea* (~25%), Poaceae (~40%) and *Artemisia* (~10%).

4.4. Sediment composition

The XRF-scanning method relies on determining the relative variations on elements composition. Nevertheless, due to the presence of major variations in organic matter or carbonates it is necessary to normalize the measured count in order to obtain an environmentally relevant signal (Löwemark et al., 2011). Aluminium and titanium normalizations are commonly used to discern possible fluctuations in the lithogenic fraction (enrichment or depletion of specific elements), particularly in the terrigenous aluminosilicate sediment fraction (Van der Weijden, 2002; Calvert and Pedersen 2007; Martinez-Ruiz et al., 2015). For this study, the XRF data were normalized to Ti since Al counts obtained were very low. Poor detection of Al can be related to either low Al content, or high organic and water contents that increase radiation absorption and affect the intensity of this light element, among other possibilities (e.g. Tjallingii et al., 2007).

Since data spacing is different between the analyses on discrete samples and the XRF scanner, a linear interpolation was performed with the purpose of equalizing the space of the different time series (150-300 years). Afterwards, the mobile average was worked out along the time series (taking into account the 5 nearest points) in order to easily identify trends by means of smoothing out data irregularities. The obtained data were compared, and both XRF-scanner and discrete sample data showed a good correlation. Consequently, the geochemical proxies displayed higher time resolution than the discrete samples (Table 2). Discrete sample and XRF data results are described together in order to simplify this section (Fig. 4).

The lower part of the core is typified by maximum values of K/Al and K/Ti ratios, coinciding with the lowest values in Ca/Al, Ca/Ti and Zr/Al ratios. Pb/Al data show a stable pattern during this interval. Nevertheless, between 10000 and 9000 cal yr BP and ~8200 cal yr BP the trends were reversed, with relatively low K/Al, low K/Ti and slightly increasing Zr/Al, Ca/Al and Ca/Ti ratios. A positive peak in Pb/Al ratio at ~8200 cal yr BP is also observed.

Between ~7000 and 4000 cal yr BP a decreasing trend in K/Al and K/Ti ratios occurs along with an increasing trend in Zr/Al, Ca/Al and Ca/Ti ratios. The Pb/Al ratio remains constant throughout this interval.

From ~4000 to ~2600 cal yr BP an increase in Zr/Al, Ca/Al and Ca/Ti ratios is documented. A maximum in eolian proxies occurs at ~2600 cal yr BP. A K/Al and K/Ti minima occurs between ~3000 and ~2600 cal yr BP. The Pb/Al ratio shows a positive peak at ~2800 cal yr BP.

The interval between ~2600 and ~1450 cal yr BP is characterized by low Ca/Al, Ca/Ti and Zr/Al ratios, with relatively high K/Al and K/Ti ratios. The Pb/Al ratio shows a flat pattern, increasing at ~1500 cal yr BP.

The period between ~1450 and ~650 cal yr BP depicts higher ratios of Zr/Al, Ca/Al and Ca/Ti and decreasing ratios of K/Al and K/Ti. A somewhat higher Pb/Al ratio is also registered during this interval.

From ~650 to ~150 low values of Zr/Al and Ca/Ti ratios and minimum values Ca/Al ratio occur. Higher K/Al and K/Ti values are also observed. The Pb/Al ratio decreases during this interval. From ~150 to the present, an increase in Zr/Al, Ca/Al, Ca/Ti, K/Ti and a Pb/Al maximum occur. Lower K/Al ratio is recorded during this period.

Several studies have demonstrated that PCA analysis of geochemical data can elucidate the importance of different geochemical components driving the environmental responses in marine and lacustrine records (Bahr et al., 2014; Yuan, 2017). We performed a PCA analysis of the LH geochemical data, which yielded two significant components (Fig. 5). The first principal component (PC1) describes 58% of the total variance. The main negative loadings for PC1 are Rb, Ba, Al, K, Ca, Mg and Sr, while large positive loadings correspond to Zr and Rare Earth Elements (REE). The second principal component (PC2) explains 17% of the total variance. The main negative loading for PC2 are Fe, Ca, Zr, Mg and Lu. Positive loads correspond to Al, K, Ba, Sr and other elements.

SEM analyses show an alternation between a lithology rich in rock fragments and another rich in organic remains. Also, diatom frustules, rich in silica, are particularly abundant since ~6300 cal yr BP to Present. Other minerals such as zircon, rounded quartz and monazite were also identified (Fig. 6).

5. Discussion

Pollen and geochemical proxies have been widely used for reconstructing vegetation changes and environmental and climate variations in southern Iberia (e.g. Carrión, 2002; Sánchez-Goñi and Fletcher, 2008; Anderson et al., 2011; Nieto-Moreno et al., 2011; Jiménez-Moreno and Anderson, 2012; Moreno et al., 2012; Fletcher and Zielhofer, 2013; Jiménez-Espejo et al., 2014; Ramos-Román et al., 2016). Variations in the occurrences of arboreal taxa such as *Pinus* and other mesic species (e.g, *Betula*, *Quercus*), indicating relative humid and warm conditions, and xerophytic species (e.g., Poaceae, Asteraceae, Amaranthaceae, *Artemisia*), representing aridity, have been useful for reconstructing relative humidity changes in southern Iberian (e.g. Carrión et al., 2001, 2007, 2010; Anderson et al., 2011; Jiménez-Moreno and Anderson, 2012; Jiménez-Moreno et al., 2013, 2015; Ramos-Román et al., 2016, 2018a, 2018b). *Pinus* reach percentages over 70% in our record. This bisaccate pollen grain is favoured by wind transport and has a larger dispersal area than other tree species, and sometimes might be overrepresented (Poska and Pidek, 2010; Pérez-Díaz et al., 2016). Nevertheless, LH is located at 2899 masl only 99 m above treeline and the upper boundary of the oromediterranean belt (1900-2800 masl) where *Pinus sylvestris* is the main tree specie (El Aallali et al., 1998; Valle, 2003). Therefore, this apparently anomalous high concentration of *Pinus* may be caused by an upward migration of the oromediterranean belt and treeline towards higher elevations and around the LH during warmer and more humid periods, which could have been overstated due to its high pollen-production and dispersal. Therefore, *Pinus* seems to be mostly recording a regional climatic signal, without allocthonous influence.

Over 75% of the total geochemical data variance is explained by the PC1 and PC2 (Fig. 5). We interpret the results of PC1 as resulting from certain sorting between heavy minerals (positive loading; Zr and REE) vs. clay minerals and feldspars (negative loadings; K, Al and Ca). The drainage basin is composed mainly by mica schist, consequently enhanced in K-rich minerals such as mica and feldspar (Díaz de Federico et al., 1980). This sorting between heavy minerals (enriched in Zr and REE) and clays and feldspars (enriched in K and Al) (Fig. 5a), was probably linked to physical weathering within the basin and to resulting runoff until final deposition in the lake.

On the other hand, we interpret the results of PC2 as differentiating autochthonous elements (positive loadings) vs. Saharan allochthonous input (negative loadings). In the first case, due to the abundance of mica schist within the LH drainage basin (Díaz de Federico et al., 1980), the K/Al and K/Ti ratios are interpreted as detrital products, and thus a proxy of runoff. In the second case, PC2 negative loading Zr, Ca, Mg and Fe (Fig. 5b) grouped elements that are coherent with Saharan input composition (dolomite, iron oxides and heavy minerals) (Ávila, 1997; Morales-Baquero et al., 2006b; Moreno et al., 2006; Pulido-Villena et al., 2007). In addition, Ca shows a strong positive correlation with Zr since 6300 cal yr BP ($r = 0.57$; $p<0.05$) supporting an eolian origin of the Ca in LH sediments. Although we cannot exclude others nearby Ca sources or changes in the source of African dust (Moreno et al., 2006), the 85% of dust reaching south Iberia derives from the Sahara (Morales-Baquero and Pérez-Martínez, 2016; Jiménez et al., 2018). For instance, enrichment in heavy minerals such as zircon and palygorskite has previously been used as an eolian proxy in the western Mediterranean (e.g., Combourieu Nebout et al., 2002, Rodrigo-Gámiz et al., 2011, 2015). High concentrations of Ca in other lacustrine systems is usually associated with biogenic sources when anti-correlated with terrigenous elements (Yuan, 2017). Nevertheless, elevated Ca in the LH record is linked with detrital elements, as shown by PC1, where Ca is associated with K and Al (Fig. 5a). Therefore Ca/Al and Ca/Ti ratios are used in the LH record as Saharan eolian input proxies.

Elemental ratio variations, such as the ratios K/Al and K/Ti indicating fluvial input and the ratios Zr/Al or Zr/Th indicating aridity and eolian input, have been previously interpreted in Alboran Sea marine records as well as in southern Iberia lake records (Martín-Puertas et al., 2010; Nieto-Moreno et al., 2011, 2015; Rodrigo-Gámiz et al., 2011; Jiménez-Espejo et al., 2014; Martínez-Ruiz et al., 2015; García-Alix et al., 2017, 2018). Thus, the integration of both palynological data and geochemical ratios used as detrital input from LH have allowed the reconstruction of the palaeoclimate and palaeoenvironmental history in Sierra Nevada during the Holocene.

5.1. Holocene palaeoclimate and palaeoenvironmental history

5.1.1. Early and Mid-Holocene humid conditions (10800–7000 cal yr BP)

The wettest conditions are recorded during the Early Holocene in Sierra Nevada. This is shown in the LH record by the highest K/Al ratio and MS values, and the low values in Zr/Al, Ca/Al and Ca/Ti ratios, suggesting that runoff dominated over eolian processes at this time (zone LH-1; Fig. 7) and agrees with previous studies in the area (Anderson et al., 2011; Jiménez-Moreno and Anderson, 2012; García-Alix et al., 2012; Jiménez-Espejo et al., 2014). Unfortunately, the pollen record from LH during this interval is insufficient to confirm this interpretation, due to the high detrital sediment composition and low organic content, as shown by the low MS values and low pollen preservation.

An Early Holocene humid stage is noticed in other nearly sites, such as the south-faced Laguna de Río Seco (LdRS; Fig. 1) (Anderson et al., 2011), when the highest lake level of the Holocene occurred. This is also coeval with the dominance of arboreal species such as *Pinus* as well as aquatic and wetland plants (Anderson et al., 2011). Low eolian input, noted by geochemical ratios, is also recorded in LdRS during this interval (Jiménez-Espejo et al., 2014). Further indications of elevated humidity come from the north-facing Borreguil de la Virgen (BdlV) (see Fig. 1), which is dominated by an AP assemblage and a high occurrence of aquatic algae *Pediastrum* along with a higher lake level (Jiménez-Moreno and Anderson, 2012).

Although the preponderance of evidence accumulated for the Early Holocene suggests overall humid conditions, at least three relatively arid periods are identified with the geochemical data in the LH record (Fig. 7). The first arid period occurred between ~9600 and 9000 cal yr BP, the second occurred ~8200 cal yr BP and the third around 7500 cal yr BP.

The first arid event is characterized in LH by a decrease in K/Al and K/Ti ratios and MS, resulting from the lower runoff input with the concomitant change to a more peaty composition. This event could be correlated with a dryness event recorded in the Siles Lake record (Carrion, 2002) at ~9300 cal yr BP noticed by an increase in *Pseudoschizaea*, which was coeval with a minor decrease in arboreal pollen also recorded in several sites in North Iberia (Iriarte-Chiapusso et al., 2016). At marine site ODP 976 (Fig.1; Combourieu-Nebout et al., 2009) a decrease in deciduous *Quercus* occurred between 9500 and 9200 cal yr BP indicating a rapid excursion towards arid conditions (Fig.7). The speleothem record of Corchia Cave also shows dryer conditions during this interval (Fig. 7; Regattieri et al., 2014) In addition, a decrease in fluvial input in the Southern Alps and an aridification phase in southeastern France and southeastern Iberia has been similarly recorded (Jalut et al., 2000).

The second dry event recorded at ~8200 cal yr BP is depicted in LH record by a negative peak in K/Ti and K/Al ratios, and by the onset of a trend toward peatier lithology as evidenced by the MS profile. This event is not recognized in LH record as clearly as the 9500 cal yr BP and the 7500 cal yr BP dry events. A decrease in *Pinus* percentage is observed in the nearby LdRS (Anderson et al., 2011), while a forest decrease is recorded in the Alboran Sea sites MD95-2043 and ODP 976. In several records from north western Iberia, a decrease in arboreal pollen also occurred at this time (Iriarte-Chiapusso et al., 2016).

The 8.2 ka event was the most rapid climate change towards cooler conditions occurred during the Holocene. It was defined in Greenland ice cores by minimum values in δ18O and affected the North Atlantic basin and the Mediterranean area (Alley et al., 1997; Rasmussen et al., 2007; Wiersma et al., 2011). Recent simulations point to a fresh water input in North Atlantic which could slow down the North Atlantic Deep Water (NADW) formation preventing the heat transport over the north hemisphere (Wiersma et al., 2010, 2011; Young et al., 2013).

Another dry event is recorded in LH at ~7500 cal yr BP evidenced by the higher peat content in the sediment, as well as by the lower MS values and a relative minimum in the K/Ti ratio. A relative AP minimum also occurred in LH at this time. This short-live event is depicted sharper than 8200 cal yr BP event in several sites in southern Iberia and Alboran Sea: In the Padul record, located at 725 masl at the lower part of Sierra Nevada a decrease in both evergreen and deciduous *Quercus* is interpreted as a dry and cold event (Ramos-Román, 2018; Ramos-Román et al., 2018a); forest expansion in Guadiana valley during the early-mid Holocene is interrupted by a xeric shrublands development between 7850 and 7390 cal yr BP (Fletcher et al., 2007); in the Alboran Sea a decrease in deciduous *Quercus* is registered at site MD95-2043; at site 300G a decrease in winter and summer temperatures is also recorded during this interval (Jiménez-Espejo et al., 2008); in lake Pergusa (south Italy) a trend toward arid conditions began at ~7500 cal yr BP (Magny et al., 2012); in Corchia Cave an arid excursion occurred at ~7500 cal yr BP within an overall humid period between 8300 cal yr BP and 7200 cal yr BP (Fig. 7; Regattieri et al., 2014).

Importantly, these arid events recorded in LH at 9600 to 9000 cal yr BP and 8200 cal yr BP are coeval with the ice-rafted debris events 6 and 5 defined by Bond et al. (1997) in North Atlantic.

5.1.2. Mid- and Late Holocene (~7000 cal yr BP-2600 cal yr BP)

The Middle and Late Holocene in the southern Iberian Peninsula is characterized by a trend towards more arid conditions (Jalut et al., 2009; Anderson et al., 2011; Rodrigo-Gámiz et al., 2011; Jiménez-Moreno and Anderson, 2012; Jiménez-Espejo et al., 2014). In the LH record an abrupt decrease in the MS values indicates a lithological change to more peaty sedimentation at ~7000 cal yr BP. Similarly, a decrease in the K/Al and K/Ti ratios, points to a transition to less humidity and runoff (Fig. 7). *Quercus* percentage increases at this time, partially replacing the *Pinus*, which mainly compose the AP during the record. A progressive increasing trend in eolian input from Sahara (Zr/Al, Ca/Al and Ca/Ti ratios) is observed around 5500-6500 cal yr BP (Fig. 7), also pointing to an increase in aridity in the area. This change coincides with regional increases in the Zr/Th ratio (equivalent to Zr/Al ratio) and *Artemisia* pollen, and with decreases in *Betula* and *Pinus* in the LdRS record (Anderson et al., 2011; Jiménez-Espejo et al., 2014), and in *Pinus* in the BdlV record (Jiménez-Moreno and Anderson, 2012). Rodrigo-Gámiz et al. (2011) and Jiménez-Espejo et al. (2014) observed similar geochemical patterns in western Mediterranean marine records and in LdRS, with a decline in fluvial input, and a decline in surface runoff, respectively. The same pattern is noticed in marine pollen records MD95-2043 and ODP 976 (Fletcher and Sanchez-Goñi, 2008; Combourieu-Nebout et al., 2009; Fig. 7). Contemporaneously, aridity is also suggested from speleothem data around the

Mediterranean area: At El Refugio cave, a hiatus in the speleothem growing rate occurred between 7300 and 6100 cal year BP (Walczak et al., 2015), which is coeval with a drop in δ18O in Soreq (Israel) and Corchia (Italy; CC26; Fig. 1 and 7) caves at 7000 cal yr BP (Bar-Matthews et al., 2000; Zanchetta et al., 2007; Regattieri et al., 2014). Also at ~7000 cal yr BP a decreasing trend in the deciduous/sclerophyllous pollen ratio occurred in southeastern France and Iberia (Jalut et al., 2000) and at continental sites around the Mediterranean Sea (Jalut et al., 2009). In addition, very low lake levels were recorded in the Sahara-Sahel Belt (Liu et al., 2007) and in the Southern Alps (Magny et al., 2002).

Enhanced arid conditions are observed in the LH record between 4000 and 2500 cal yr BP, interpreted through a decline in AP and a Poaceae maximum. Also a surface runoff minimum and an increase in eolian input proxies took place between 3500 and 2500 cal yr BP (zone LH-3). In Corchia Cave an arid interval was recorded at ~3100 cal yr BP (Regattieri et al., 2014), coeval with another one observed globally and described by Mayewski et al. (2004) between 3500 and 2500 cal yr BP. Nevertheless, this period is not climatically stable, fluctuations are observed in in K/Ti, K/Al, Ca/Ti, Ca/Al and Zr/Al ratios. Furthermore, peaks in *Quercus* are recorded in LH, LdlM and ODP 976 sites at ~3900 cal yr BP and ~3100 cal yr BP, when AP in LH decreases (Combourieu-Nebout et al., 2009; Jiménez-Moreno et al., 2013). This fact a priori contradictory, could be explained by altitudinal displacements of the tree taxa such as *Quercus* in the oromediterranean belt due to the climatic variability occurred along this interval (Carrión, 2002). During warmer periods, this species would be displaced towards higher elevation and the influence of *Quercus* pollen in Sierra Nevada would be larger, this could explain relative higher *Quercus* percentages in LdlM, LH and also in the ODP 976 record. The same relationship between *Quercus* and *Pinus* is observed comparing the BdlC and Padul records, located closely but with large altitude difference (BdlC ~2992 masl; Padul ~725 masl; Ramos-Román, 2018) where is also likely linked to movements in the oromediterranean belt (Ramos-Román, 2018). These altitudinal displacements of the tree taxa have been previously related to temperature changes in others southern Iberian records, suggesting an ecological niche competition between *Pinus* and *Quercus* species at middle altitudes (see Carrión et al., 2002 for a revision).

5.1.3. Iberian Roman Humid Period (IRHP; ~2600-1450 cal yr BP)

Because there is no consensus in the literature about the chronology for the main climatic stages during the last 2000 years (Muñoz-Sobrino et al., 2014; Helama et al., 2017), here we follow the chronology proposed by Moreno et al. (2012): Dark Ages (DA, 1450-1050 cal yr BP); Medieval Climate Anomaly (MCA, 1050-650 cal yr BP); and LIA (650-150 cal yr BP). Another climatic stage preceeds the DA – the Iberian Roman Humid Period (IRHP, 2600-1600 cal yr BP), originally described by Martín-Puertas et al. (2008). However, in the LH record we have established different IRHP limits (2600-1450), based accordingly to the pollen zonation (Fig. 3), and coinciding with the DA onset defined by Moreno et al, (2012).

The IRHP has been described as the wettest period in the western Mediterranean from proxies determined both in marine and lacustrine records during the Late Holocene (Reed et al., 2001; Fletcher and Sanchez-Goñi 2008; Combourieu-Nebout et al., 2009; Martín-Puertas et al., 2009; Nieto-Moreno et al., 2013; Sánchez-López et al., 2016). A relative maximum in AP occurred in the LH record during this time, also indicating forest development and relative high humidity during the Late Holocene in the area (zone LH-4; Fig. 7). This is further supported by high K/Al and K/Ti ratios and MS values, indicating high detrital input in the drainage basin, a minimum in Poaceae and low Saharan eolian input (low Ca/Al, Ca/Ti and

Zr/Al ratios) (Fig. 7). Fluvial elemental ratios have also shown an increase in river runoff in Alboran Sea marine records (Nieto-Moreno et al., 2011; Rodrigo-Gámiz et al., 2011). This humid period seems to be correlated with a solar maximum (Solanki et al., 2004) and persistent negative NAO conditions (Olsen et al., 2012), which could have triggered general humid conditions in the Mediterranean. However, in the LH record fluctuation in AP between 2300 and 1800 cal yr BP occurred, pointing to arid conditions at that time. This arid event also seems to show up in BdlC, with a decrease in AP between 2400 and 1900 cal yr BP (Ramos-Román et al., 2016) and in Zoñar Lake, with water highly chemically concentrated and gypsum deposition between 2140 and 1800 cal yr BP (Martín-Puertas et al., 2009). In Corchia Cave a rapid excursion towards arid condition is recoded at ~2000 cal yr BP (Regattieri et al., 2014) (Fig.7). As we explained in section 5, the apparently anomalous percentages of *Pinus* at this time, could be justified by an upward migrations of the oromediterranean forest species triggered by higher temperatures and/or the high pollen-production and dispersal of *Pinus*. Nevertheless, we cannot exclude others factors that could influence the pollen transport such as the wind energy, mostly controlled by the NAO in the southern Iberia. A persistent negative NAO phase, as occurred during the IRWP (Sánchez-López et al., 2016), would have triggered more humid conditions and higher westerlies influence over southern Europe. The higher occurrence of *Pinus* in the surrounding area due to the favourable climatic conditions, along with the higher wind energy over Sierra Nevada and the characteristics of bissacate pollen, could have overstate the percentages of *Pinus* in our record.

5.1.4. Dark Ages and Medieval Climate Anomaly (DA, MCA; 1450-650 cal yr BP)

Predominantly arid conditions, depicted by high abundance of herbaceous and xerophytic species and an AP minimum in the LH record, are shown for both DA and MCA (zone LH-5; Fig. 7). This is further supported in this record by an increase in Saharan eolian input Ca/Al, Ca/Ti and Zr/Al ratios, and by a decrease in surface runoff, indicated by the K/Al and K/Ti ratios (zone LH-5; Fig. 7). These results from LH agree with climate estimations of overall aridity modulated by a persistent positive NAO phase during this period (Trouet et al., 2009; Olsen et al., 2012), also previously noted by Ramos-Román et al. (2016) in the area (Fig. 7).

Generally arid climate conditions during the DA and the MCA have also been previously described in the LdlM and BdlC records, shown by a decrease in mesophytes and a rise of xerophytic vegetation during that time (Jiménez-Moreno et al., 2013; Ramos-Román et al., 2016). Several pollen records in south and central Iberian Peninsula also indicate aridity during the DA and MCA, for example grassland expanded at Cañada de la Cruz, while in Siles Lake a lower occurrence of woodlands occurred (Carrión, 2002). Also in Cimera Lake low lake level and higher occurrence of xerophytes were recorded (Sánchez-López et al., 2016). Arid conditions were depicted in Zoñar Lake by an increase in *Pistacia* and heliophytes (i.e., Chenopodiaceae) and lower lake level (Martín-Puertas et al., 2010). Similar climatic conditions were noticed in the marine records MD95-2043 and ODP 976 in the Alboran Sea through decreases in forest (Fletcher and Sánchez-Goñi, 2008; Combourieu-Nebout et al., 2009; Fig. 7). Arid conditions in Basa de la Mora (northern Iberian Peninsula) occurred during this time, characterized by maximum values of *Artemisia*, and a lower development of deciduous *Quercus* and aquatic species such as *Potamogeton*, also indicating low lake water levels (Moreno et al., 2012). Arid conditions were also documented by geochemical data in marine records from the Alboran Sea (Nieto-Moreno et al., 2013, 2015), in the Gulf of Lion and South of Sicily (Jalut et al., 2009). Aridity has also been interpreted for central Europe using lake level reconstructions (Magny, 2004) and in speleothems records in central Italy (Regattieri et al., 2014). Nevertheless, wetter conditions were recorded during the DA in some records from northern Iberian Peninsula (Sánchez-López et al., 2016). Humid conditions depicted by higher lake level and less salinity occurred in Arreo Lake (Corella et al., 2013). In Sanabria Lake, the dominance of planktonic diatom *Aulacoseira subborealis* is interpreted as relative humid conditions at that time (Jambrina-Enríquez et al., 2014). This heterogeneity in the climate during the DA is due to the existence of an N-S humidity gradient in the Iberian Peninsula (Sánchez-López et al., 2016). Nonetheless, this gradient seems to be more diffuse during the MCA, which is characterized as an overall arid period in the entire Iberian Peninsula (Morellón et al., 2012; Sánchez-López et al., 2016).

5.1.5. Little Ice Age (LIA; 650-150 cal yr BP)

The LIA is interpreted as an overall humid period in the LH record. This is indicated by higher AP values than during the MCA, low Saharan dust input (low Ca/Al, Ca/Ti and Zr/Al ratios), a decrease in herbs (Poaceae) and high values in the K/Al and K/Ti ratios indicating enhanced runoff (zone LH-6A; Fig. 7). An increase in fluvial-derived proxies has been previously documented in other Iberian terrestrial records such as Basa de la Mora Lake (Moreno et al., 2012), Zoñar Lake (Martín-Puertas et al., 2010) or Cimera Lake (Sánchez-López et al., 2016) and marine records from the Alboran Sea basin (Nieto-Moreno et al., 2011, 2015). Lake level reconstructions in Estanya Lake, in the Pre-Pyrenees (NE Spain), have shown high water levels during this period (Morellón et al., 2009, 2011), supporting our humid climate inferences. Nevertheless, fluctuations in *Artemisia* during the LIA suggest an unstable period in Sierra Nevada (Fig. 8), in agreement with the high variability in *Pinus*, *Artemisia*, and water availability deduced from recent high-resolution studies in the neighbour BdlC and BdlV records (Ramos-Román et al., 2016; García-Alix et al., 2017). The same pattern occurred in several Iberian records (Oliva et al., 2018), revealing that the LIA was not a climatically stable period and many oscillations at short-time scale occurred.

A persistently negative NAO phase, although with high variability, occurred during this period (Trouet et al., 2009), which could explain the overall humid conditions observed in southern Europe. As in the Early Holocene arid events, solar variability has been hypothesized as the main forcing of this climatic event (Bond et al., 2001; Mayewski et al., 2004; Fletcher et al., 2013; Ramos-Román et al., 2016).

5.2. Industrial Period (IP; 150 cal yr BP-Present)

The IP is characterized by a sharp increase in the Pb/Al ratio in LH record(Fig. 8), suggesting more mining, fossil fuel burning or other human industrial activities (García-Alix et al., 2013, 2017). This is coeval with a rise in AP, which is also related to human activities such as *Olea* commercial cultivation at lower elevations around Sierra Nevada or *Pinus* reforestation in the area (Fig. 7 and 8; Valbuena-Carabaña et al., 2010; Anderson et al., 2011). The same pattern has also been observed in others records from Sierra Nevada (Jiménez-Moreno and Anderson, 2012; García-Alix et al., 2013; Ramos-Román et al., 2016), in Zoñar Lake and the Alboran Sea records (Martín-Puertas et al., 2010). In addition, a progressively increasing trend in Zr/Al and Ca/Al ratios is observed during the last two centuries, which could be related to increasing local aridity and/or anthropogenic desertification, but also with a change in the origin and/or composition of the dust reaching to the lake (Jiménez-Espejo et al., 2014), likely related to the beginning of extensive agriculture and the concomitant desertification in the Sahel region (Mulitza et al., 2010).

5.3 Significance of the eolian record from Laguna Hondera

Saharan dust influence over current alpine lake ecosystems is widely known (Morales-Baquero et al., 2006a, 2006b; Pulido-Villena et al., 2008b; Mladenov et al., 2011, Jiménez et al., 2018). The most representative elements of Saharan dust in LH record are Fe, Zr and Ca as shown by the PC2 loading (Fig. 5), where Ca and Fe directly affect the alpine lake biogeochemistry in this region (Pulido-Villena et al., 2006, 2008b, Jiménez et al., 2018). Zirconium is transported in heavy minerals in eolian dust (Govin et al., 2012) and has largely been used in the Iberian Peninsula and the western Mediterranean as an indicator of eolian Saharan input (Moreno et al., 2006; Nieto-Moreno et al., 2011; Rodrigo-Gámiz et al., 2011; Jiménez-Espejo et al., 2014; Martínez-Ruiz et al., 2015, and references therein). High Zr content has also been identified in present aerosols at high elevations in Sierra Nevada (García-Alix et al., 2017). Considering the low weatherable base cation reserves in LH bedrock catchment area, calcium is suggested to be carried by atmospheric input of Saharan dust into alpine lakes in Sierra Nevada (Pulido-Villena et al., 2006, see discussion; Morales-Baquero et al., 2013). This is the first time that the Ca signal is properly recorded in a long record from Sierra Nevada. This could be explained by higher evaporation rates at this site promoting annual lake desiccation that could prevent Ca water column dissolution and using/recycling by organism, preserving better the original eolian signal. These elements have an essential role as nutrients becoming winnowed and recycled rapidly in the oligotrophic alpine lake ecosystem (Morales-Baquero et al., 2006b). This phenomenon has also been observed in other high-elevation lakes where the phytoplankton is supported by a small and continually recycled nutrient pool (e.g., Sawatzky et al., 2006).

The SEM observations further confirm the presence of Saharan dust in the lake sediments from LH and the occurrence of Zircon, the main source of eolian Zr, which is relatively abundant (Fig. 6a). Quartz with rounded morphologies (eolian erosion) are also frequent (Fig. 6b) in the uppermost part of the record as well as REE rich minerals, such as monazite, which is typical from the Saharan-Sahel Corridor area (Moreno et al., 2006) (Fig. 6c). In addition, the fact that the highest correlation between Ca and Zr occurred after ~6300 cal yr BP, ($r=0.57$ $p<0.005$) along with the SEM observation and the low availability of Ca in these ecosystems, could suggest that the beginning of Saharan dust arrivals to the lake, including both elements, took place at this time, giving rise to the present way of nutrient inputs in these alpine lakes (Morales-Baquero et al., 2006b; Pulido-Villena et al., 2006). The onset of Saharan dust input into southern Iberia occurred prior to the end of the African Humid Period (AHP; ~5500 cal yr BP; deMenocal et al., 2000), as previously noticed in the nearby LdRS (Jiménez-Espejo et al., 2014) and in Alboran Sea (Rodrigo-Gámiz et al., 2011). This could suggest a progressive climatic deterioration in North Africa, which culminated with the AHP demise and the massive Saharan dust input recorded in all records in Sierra Nevada at ~3500 cal yr BP (Fig. 7).

6. Conclusions

The multiproxy paleoclimate analysis from LH has allowed the reconstruction of the vegetation and climate evolution in Sierra Nevada and southern Iberia during the Holocene, and the possible factors that have triggered paleoenvironmental changes. Climate during the Early Holocene was predominantly humid, with two relatively arid periods between 10000 and 9000 and at ~8200 cal yr BP, resulting in less detrital inputs and a change to more peaty lithology. The onset of an arid trend took place around 7000 cal yr BP, decreasing the runoff input in the area. A significant increase in eolian-derived elements occurred between 6300 and 5500 cal yr BP, coinciding with the AHP demise. An arid interval is recorded between 4000 and 2500 cal yr BP, with a vegetation assemblage dominated by xerophytes.

Relative humid conditions occurred in the area between 2500 and 1450 cal yr BP, interrupting the Late Holocene aridification trend. This humid interval was characterized by expansion of forest vegetation, high runoff input, and a more clayey lithology. However, during the DA and the MCA (1450-650 cal yr BP) there was enhanced eolian input and an expansion of xerophytes, indicating increased arid conditions. In contrast, the LIA (650-150 cal yr BP) was characterized by predominant humid conditions as pointed out high runoff and low eolian input. The IP (150 cal yr BP-Present) is characterized in the LH record by the highest values of the Pb/Al ratio, probably indicating fossil fuel burning by enhanced mining and metallurgy industry. The increase in human activities at this time in this area can also be deduced by the expansion of *Olea* cultivation at lower elevations and *Pinus* reforestation in the area.

Importantly, the LH record shows a unique and exceptional Ca signal derived from eolian input (high Ca-Zr correlation) during the past ~6300 years in Sierra Nevada. The good preservation of the Ca record might have been favoured by the high evaporation and the low lake depth, which could have prevented Ca column water dissolution and its re-use by organisms. Our record indicate that present-day inorganic nutrient input from Sahara was established 6300 yrs ago and lasted until the present, with variations depending on the prevailing climate.

Acknowledgements

This study was supported by the project P11-RNM 7332 of the "Junta de Andalucía", the projects CGL2013-47038-R, CGL2015-66830-R of the "Ministerio de Economía y Competitividad of Spain and Fondo Europeo de Desarrollo Regional FEDER", the research groups RNM0190 and RNM179 (Junta de Andalucía). We also thank to Unidad de Excelencia (UCE-PP2016-05). J.M.M.F acknowledges the PhD funding provided by Ministerio de Economía y Competitividad (CGL2015-66830-R) A.G.-A. was also supported by a Marie Curie Intra-European Fellowship of the 7th Framework Programme for Research, Technological Development and Demonstration of the European Commission (NAOSIPUK. Grant Number: PIEF-GA-2012-623027) and by a Ramón y Cajal Fellowship RYC-2015-18966 of the Spanish Government (Ministerio de Economía y Competividad) and M.R.G. from the Andalucía Talent Hub Program co-funded by the European Union's Seventh Framework Program (COFUND – Grant Agreement nº 291780) and the Junta de Andalucía. We thank Santiago Fernández, Maria Dolores Hernandez and Antonio Mudarra for their help recovering the core and Inés Morales for the initial core description and MS data. We thank Jaime Frigola (Universitat de Barcelona) for his help with XRF core scanning.

References

Anderson, R. S., Jiménez-Moreno, G., Carrión, J. S., and Pérez-Martínez, C.: Holocene vegetation history from Laguna de Río Seco, Sierra Nevada, southern Spain, Quaternary Sci. Rev. 30, 1615-1629, DOI:10.1016/j.quascirev.2011.03.005, 2011.

Andrade, A., Valdeolmillos, A., and Ruíz-Zapata, B.: Modern pollen spectra and contemporary vegetation in the Paramera Mountain range (Ávila, Spain), Rev. Palaeobot. Palyno., 82, 127-139, DOI:10.1016/0034-6667(94)90024-8, 1994.

Ariztegui, D., Asioli, A., Lowe, J. J., Trincardi, F., Vigliotti, L., Tamburini, F., Chondrogianni, C., Accorsi, C. A., Bandini Mazzanti, M., Mercuri, A. M., Van der Kaars, S., McKenzie, J. A., and Oldfield, F.: Palaeoclimate and the formation of sapropel S1: inferences from Late Quaternary lacustrine and marine sequences in the central Mediterranean region, Palaeogeogr. Palaeocl., 158, 215-240, DOI:10.1016/S0031-0182(00)00051-1, 2000.

Aubet, M. E.: The Phoenicians and the West: Politics, colonies and trade, Cambridge University Press, Cambridge, 2001.

Ávila, A., Queralt-Mitjans, I., and Alarcón, M.: Mineralogical composition of African dust delivered by red rains over northeastern Spain, J. Geophys. Res.-Atmos., 102, 21977-21996, DOI:10.1029/97JD00485, 1997.

Ballantyne, A. P., Brahney, J., Fernandez, D., Lawrence, C. L., Saros, J., and Neff, J. C.: Biogeochemical response of alpine lakes to a recent increase in dust deposition in the Southwestern US, Biogeosciences, 8, 2689, DOI:10.5194/bg-8-2689-2011, 2011.

Bar-Matthews, M., Ayalon, A., and Kaufman, A.: Timing and hydrological conditions of sapropel events in the Eastern Mediterranean, as evident from speleothems, Soreq cave, Israel, Chem. Geol., 169, 145-156, DOI:10.1016/S0009-2541(99)00232-6, 2000.

Bahr, A., Jiménez-Espejo, F. J., Kolasinac, N., Grunert, P., Hernández-Molina, F. J., Röhl, U., Voelker, A. H. L., Escutia, C., Stow, D. A. V., Hodell, D., and Alvarez-Zarikian, C. A.: Deciphering bottom current velocity and paleoclimate signals from contourite deposits in the Gulf of Cádiz during the last 140 kyr: An inorganic geochemical approach, Geochem. Geophy. Geosy., 15, 3145-3160, DOI:10.1002/2014GC005356, 2014.

Blaauw, M.: Methods and code for ‘classical’ age-modelling of radiocarbon sequences, Quat. Geochronol., 5, 512-518, DOI:10.1016/j.quageo.2010.01.002, 2010.

Bea, F.: Residence of REE, Y, Th and U in granites and crustal protoliths: implications for the chemistry of crustal melts, J. Petrol., 37, 521-532, DOI:10.1093/petrology/37.3.521, 1996.

Beug, H. J.: Leitfaden der Pollenbestimmung für Mitteleuropa und angrenzende Gebiete, Fischer, Stuttgart, 2004.

Bond, G., Showers, W., Cheseby, M., Lotti, R., Almasi, P., deMenocal, P., Priore, P., Cullen, H., Hajdas, I., and Bonani, G.: A pervasive millennial-scale cycle in North Atlantic Holocene and glacial climates, Science, 278, 1257-1266, DOI:10.1126/science.278.5341.1257, 1997.

Bond, G., Kromer, B., Beer, J., Muscheler, R., Evans, M., Showers, W., Hoffmann, S., Lotti-Bond, R., Hajdas, I., and Bonani, G.: Persistent solar influence on North Atlantic climate during the Holocene, Science, 294, 2130-2136, DOI:10.1126/science.1065680, 2001.

Cacho, I., Grimalt, J. O., and Canals, M.: Response of the Western Mediterranean Sea to rapid climatic variability during the last 50,000 years: a molecular biomarker approach, J. Marine Syst., 33-34, 253-272, DOI:10.1016/S0924-7963(02)00061-1, 2002.

Calvert, S. E., and Pedersen, T. F.: Elemental proxies for palaeoclimatic and palaeoceanographic variability in marine sediments: interpretation and application, Proxies in Late Cenozoic Paleoceanography, Elsevier, Amsterdam, 2007.

Carrión, J. S.: Patterns and processes of Late Quaternary environmental change in a montane region of southwestern Europe, Quaternary Sci. Rev., 21, 2047-2066, DOI:10.1016/S0277-3791(02)00010-0, 2002.

Carrión, J. S., Munuera, M., Dupré, M., and Andrade, A.: Abrupt vegetation changes in the Segura mountains of southern Spain throughout the Holocene, J. Ecol., 89, 783-797, DOI:10.1046/j.0022-0477.2001.00601.x, 2001.

Carrión, J. S., Sánchez-Gómez, P., Mota, J. F., Yll, E. I., and Chaín, C.: Fire and grazing are contigent on the Holocene vegetation dynamics of Sierra de Gádor, southern Spain, Holocene 13, 839-849, DOI:10.1191/0959683603hl662rp, 2003.

Carrión, J. S., Fuentes, N., González-Sampériz, P., Sánchez Quirante, L., Finlayson, J. C., Fernández, S., and Andrade, A.: Holocene environmental change in a montane region of sourthern Europe with a long history of human settlement, Quaternary Sci. Rev., 26, 1455-1475, DOI:10.1016/j.quascirev.2007.03.013, 2007.

Carrión, J. S., Fernández, S., González-Sampériz, P., Gil-Romera, G., Badal, E., Carrión-Marco, Y., López-Merino, L., López-Sáez, J. A., Fierro, E., and Burjachs, F.: Expected trends and surprises in the Lateglacial and Holocene vegetation history of the Iberian Peninsula and Balearic Islands, Rev. Palaeobot. Palyno., 162, 458-476, DOI:10.1016/j.jaridenv.2008.11.014, 2010.

Castillo Martín, A.: Lagunas de Sierra Nevada, Universidad de Granada, Granada, 2009.

Combourieu Nebout, N., Turon, J. L., Zahn, R., Capotondi, L., Londeix, L., and Pahnke, K.: Enhanced aridity and atmospheric high-pressure stability over the western Mediterranean during the North Atlantic cold events of the past 50 ky, Geology, 30, 863-866, DOI:10.1130/0091-7613(2002)030<0863:EAAAHP>2.0.CO;2 , 2002..

Combourieu Nebout, N., Peyron, O., Dormoy, I., Desprat, S., Beaudouin, C., Kotthoff, U., and Marret, F.: Rapid climatic variability in the west Mediterranean during the last 25,000 years from high resolution pollen data, Clim. Past, 5, 503-521, DOI:10.5194/cpd-5-671-2009, 2009.

Comero, S., Locoro, G., Free, G., Vaccaro, S., De Capitani, L., and Gawlik, B. M.: Characterisation of Alpine lake sediments using multivariate statistical techniques, Chemometr. Intell. Lab., 107(1), 24-30, DOI:10.1016/j.chemolab.2011.01.002, 2011.

Corella, J. P., Stefanova, V., El Anjoumi, A., Rico, E., Giralt, S., Moreno, A., Plata-Monter, A., and Valero-Garcés, B. L.: A 2500-year multi-proxy reconstruction of climate change and human activities in northern Spain: the Lake Arreo record, Palaeogeogr. Palaeoclimatol. Palaeoecol., 386, 555-568, DOI:10.1016/j.palaeo.2013.06.022, 2013.

Davis, J. C., and Sampson, R. J.: Statistics and data analysis in geology, Willey, New York, 1986.

de Lange, G. J., Thomson, J., Reitz, A., Slomp, C. P., Principato, M. S., Erba, E., and Corselli, C.: Synchronous basin-wide formation and redox-controlled preservation of a Mediterranean sapropel, Nat. Geosci., 1, 606-610, DOI:10.1038/ngeo283, 2008.

deMenocal, P., Ortiz, J., Guilderson, T., Adkins, J., Sarnthein, M., Baker, L., and Yarusinsky, M.: Abrupt onset and termination of the African Humid Period: rapid climate responses to gradual insolation forcing, Quaternary Sci. Rev., 19, 347-361, DOI:10.1016/S0277-3791(99)00081-5, 2000.

Díaz de Federico, A.: Estudio geológico del Complejo de Sierra Nevada en la transversal del Puerto de la Ragua (Cordillera Bética), Ph.D. thesis, Universidad de Granada, Granada, 1980.

El Aallali, A., López Nieto, J. M., Pérez Raya, F., and Molero Mesa, J.: Estudio de la vegetación forestal en la vertiente sur de Sierra Nevada (Alpujarra Alta granadina), Itinera Geobot., 11, 387-402, 1998.

Faegri, K., and Iversen, J.: Textbook of Pollen Analysis, Wiley, New York, 1989.

Fletcher, W. J., Boski, T., and Moura, D.: Palynological evidence for environmental and climatic change in the lower Guadiana valley, Portugal, during the last 13 000 years, Holocene, 17, 481-494, DOI:10.1177/0959683607077027, 2007.

Fletcher, W. J., and Sánchez Goñi, M. F.: Orbital- and sub-orbital-scale climate impacts on vegetation of the western Mediterranean basin over the last 48,000 yr, Quaternary Res., 70, 451-464, DOI:10.1016/j.yqres.2008.07.002, 2008.

Fletcher, W. J., Sánchez Goñi, M. F., Peyron, O., and Dormoy, I.: Abrupt climate changes of the last deglaciation detected in a Western Mediterranean forest record, Clim. Past, 6, 245-264, DOI:10.5194/cp-6-245-2010, 2010.

Fletcher, W. J., and Zielhofer, C.: Fragility of Western Mediterranean landscapes during Holocene rapid climate changes, Catena, 103, 16-29, DOI:10.1016/j.catena.2011.05.001, 2013.

García-Alix, A., Jiménez-Moreno, G., Anderson, R. S., Jiménez-Espejo, F. J., and Delgado-Huertas, A.: Holocene paleoenvironmental evolution of a high-elevation wetland in Sierra Nevada, southern Spain, deduced from an isotopic record, J. Paleolimnol., 48, 471-484, DOI:10.1007/s10933-012-9625-2 , 2012.

García-Alix, A., Jiménez-Espejo, F. J., Lozano, J. A., Jiménez-Moreno, G., Martinez-Ruiz, F., García Sanjuán, L., Aranda Jiménez, G., García Alfonso, E., Ruiz-Puertas, G., and Anderson, R. S.: Anthropogenic impact and lead pollution throughout the Holocene in Southern Iberia, Sci. Total Environ., 449, 451-460, DOI:10.1016/j.scitotenv.2013.01.081, 2013.

García-Alix, A., Jimenez Espejo, F. J., Toney, J. L., Jiménez-Moreno, G., Ramos-Román, M. J., Anderson, R. S., Ruano, P., Queralt, I., Delgado Huertas, A., and Kuroda, J.: Alpine bogs of southern Spain show human-induced environmental change superimposed on long-term natural variations, Sci. Rep.-UK, 7, 7439, DOI:10.1038/s41598-017-07854-w, 2017.

García-Alix, A., Jiménez-Espejo, F.J., Jiménez-Moreno, G., Toney, J.L., Ramos-Román, M.J., Camuera, J., Anderson, R.S., Delgado-Huertas, A., Martínez-Ruiz, F., and Queralt, I.: Holocene geochemical footprint from Semi-arid alpine wetlands in southern Spain, Sci. Data, 5, 180024, DOI:10.1038/sdata.2018.24, 2018.

Govin, A., Holzwarth, U., Heslop, D., Ford Keeling, L., Zabel, M., Mulitza, S., Collins, J. A., and Chiessi, C. M.: Distribution of major elements in Atlantic surface sediments (36ºN-49ºS): imprint of terrigenous input and continental weathering, Geochem. Geophy. Geosy., 13, Q01013, DOI:10.1029/2011GC003785, 2012.

Grimm, E. C.: CONISS: a Fortran 77 program for stratigraphically constrained cluster analysis by the method of incremental sum of squares, Comput. Geosci., 13, 13-35, DOI:10.1016/0098-3004(87)90022-7, 1987.

Grimm, E.: TILIA: a pollen program for analysis and display, Illinois State Museum, Springfield, 1993.

Hammer, Ø., Harper, D. A. T., and Ryan, P. D.: Paleontological Statistics Software Package for Education and Data Analysis, Palaeontol. electron., 4, 1-9, 2001.

Harper, D. A. T.: Numerical Palaeobiology, John Wiley & Sons, Chichester, 1999.

Helama, S., Jones, P. D., and Briffa, K. R.: Dark Ages Cold Period: A literature review and directions for future research, Holocene 27, 1600-1606, DOI: 10.1177/0959683617693898, 2017.

Jalut, G., Esteban Amat, A., Bonnet, L., Gauquelin, T., and Fontugne, M.: Holocene climatic changes in the Western Mediterranean, from south-east France to south-east Spain, Palaeogeogr. Palaeocl., 160, 255-290, DOI:10.1016/S0031-0182(00)00075-4, 2000.

Jalut, G., Dedoubat, J. J., Fontugne, M., and Otto, T.: Holocene circum-Mediterranean vegetation changes: climate forcing and human impact, Quatern. Int., 200, 4-18, DOI:10.1016/j.quaint.2008.03.012, 2009.

Jambrina-Enríquez, M., Rico, M., Moreno, A., Leira, M., Bernárdez, P., Prego, R., Recio, C., and Valero-Garcés, B. L.: Timing of deglaciation and postglacial environmental dynamics in NW Iberia: the Sanabria Lake record, Quaternary Sci. Rev., 94, 136-158, DOI:10.1016/j.quascirev.2014.04.018, 2014.

Jiménez, L., Rühland, K. M., Jeziorski, A., Smol, J. P., and Pérez-Martínez, C.: Climate change and Saharan dust drive recent cladoceran and primary production changes in remote alpine lakes of Sierra Nevada, Spain, Glob. Change Biol., 24, e139-e158, DOI:10.1111/gcb.13878, 2018.

Jiménez-Espejo, F. J., Martínez-Ruiz, F., Rogerson, M., González-Donoso, J. M., Romero, O., Linares, D., Sakamoto, T., Gallego-Torres, D., Rueda Ruiz, J. L., Ortega-Huertas, M., and Perez Claros, J. A.: Detrital input, productivity fluctuations, and water mass circulation in the westernmost Mediterranean Sea since the Last Glacial Maximum, Geochem. Geophy. Geosy., 9, Q11U02, DOI:10.1029/2008GC002096, 2008.

Jiménez-Espejo, F. J., García-Alix, A., Jiménez-Moreno, G., Rodrigo-Gámiz, M., Anderson, R. S., Rodríguez-Tovar, F. J., Martínez-Ruiz, F., Giralt, S., Delgado-Huertas, A., and Pardo-Igúzquiza, E.: Saharan aeolian input and effective humidity variations over western Europe during the Holocene from a high altitude record, Chem. Geol., 374, 1-12, DOI:10.1016/j.chemgeo.2014.03.001, 2014.

Jiménez-Moreno, G., and Anderson, R. S.: Holocene vegetation and climate change recorded in alpine bog sediments from the Borreguiles de la Virgen, Sierra Nevada, southern Spain, Quaternary Res., 77, 44-53, DOI:10.1016/j.yqres.2011.09.006, 2012.

Jiménez-Moreno, G., García-Alix, A., Hernández-Corbalán, M. D., Anderson, R. S., and Delgado-Huertas, A.: Vegetation, fire, climate and human disturbance history in the southwestern Mediterranean area during the late Holocene, Quaternary Res., 79, 110-122, DOI:10.1016/j.yqres.2012.11.008, 2013.

Jiménez-Moreno, G., Rodríguez-Ramírez, A., Pérez-Asensio, J. N., Carrión, J. S., López-Sáez, J. A., Villarías-Robles, J. J. R., Celestino-Pérez, S., Cerrillo-Cuenca, E., Ángel León, A., and Contreras, C.: Impact of late-Holocene aridification trend, climate variability and geodynamic control on the environment from a coastal area in SW Spain, Holocene, 25, 607-617, DOI:10.1177/0959683614565955, 2015.

Lionello, P., Malanotte-Rizzoli, P., Boscolo, R., Alpert, P., Artale, V., Li, L., Luterbacher, J., May, W., Trigo, R., Tsimplis, M., Ulbrich, U., and Xoplaki, E.: The Mediterranean climate: an overview of the main characteristics and issues, Developments in Earth and Environmental Sciences, 4, Elsevier, Amsterdam, Netherlands, 1-26, 2006.

Liu, Z., Wang, Y., Gallimore, R., Gasse, F., Johnson, T., deMenocal, P., Adkins, J., Notaro, M., Prentice, I. C., Kutzbach, J., Jacob, R., Behling, P., Wang, L., and Ong, E.: Simulating the transient evolution and abrupt change of Northern Africa atmosphere–ocean–terrestrial ecosystem in the Holocene. Quaternary Sci. Rev., 26, 1818-1837, DOI:10.1016/j.quascirev.2007.03.002, 2007.

Löwemark, L., Chen, H.-F., Yang, T.-N., Kylander, M., Yu, E.-F., Hsu, Y.-W., Lee, T.-Q., Song, S.-R., and Jarvis, S.: Normalizing XRF-scanner data: a cautionary note on the interpretation of high-resolution records from organic-rich lakes, J. Asian Earth Sci., 40, 1250-1256, DOI:10.1016/j.jseaes.2010.06.002, 2011.

Magny, M., Miramont, C., and Sivan, O.: Assessment of the impact of climate and anthropogenic factors on Holocene Mediterranean vegetation in Europe on the basis of palaeohydrological records, Palaeogeogr. Palaeocl., 186, 47-59, DOI:10.1016/S0031-0182(02)00442-X, 2002.

Magny, M., and Bégeot, C.: Hydrological changes in the European midlatitudes associated with freshwater outbursts from Lake Agassiz during the Younger Dryas event and the early Holocene, Quaternary Res., 61, 181-192, doi:10.1016/j.yqres.2003.12.003, 2004.

Magny, M., de Beaulieu, J.-L., Drescher-Schneider, R., Vannière, B., Walter-Simonnet, A.-V., Miras, Y., Millet, L., Bossuet, G., Peyron, O., Brugiapaglia, E., and Leroux, A.: Holocene climate changes in the central Mediterranean as recorded by lake-level fluctuations at Lake Accesa (Tuscany, Italy), Quaternary Sci. Rev., 26, 1736-1758, DOI:10.1016/j.quascirev.2007.04.014, 2007.

Magny, M., Peyron, O., Sadori, L., Ortu, E., Zanchetta, G., Vannière, B., and Tinner, W.: Contrasting patterns of precipitation seasonality during the Holocene in the south- and north-central Mediterranean, J. Quat. Sci., 27, 290-296, DOI:10.1002/jqs.1543, 2012.

Martín-Puertas, C., Valero-Garcés, B. L., Mata, M. P., González-Sampériz, P., Bao, R., Moreno, A., and Stefanova, V.: Arid and humid phases in southern Spain during the last 4000 years: the Zonar Lake record, Cordoba, Holocene, 18, 907-921, DOI:10.1177/0959683608093533, 2008.

Martín-Puertas, C., Valero-Garcés, B. L., Brauer, A., Mata, M. P., Delgado-Huertas, A., and Dulski, P.: The Iberian–Roman Humid Period (2600–1600 cal yr BP) in the Zoñar Lake varve record (Andalucía, southern Spain), Quaternary Res., 71, 108-120, DOI:10.1016/j.yqres.2008.10.004, 2009.

Martín-Puertas, C., Jiménez-Espejo, F., Martínez-Ruiz, F., Nieto-Moreno, V., Rodrigo, M., Mata, M. P., and Valero-Garcés, B. L.: Late Holocene climate variability in the southwestern Mediterranean region: an integrated marine and terrestrial geochemical approach, Clim. Past, 6, 807-816, DOI:10.5194/cp-6-807-2010, 2010.

Martínez-Ruiz, F., Kastner, M., Gallego-Torres, D., Rodrigo-Gámiz, M., Nieto-Moreno, V., and Ortega-Huertas, M.: Paleoclimate and paleoceanography over the past 20,000 yr in the Mediterranean Sea Basins as indicated by sediment elemental proxies, Quaternary Sci. Rev., 107, 25-46, DOI:10.1016/j.quascirev.2014.09.018, 2015.

Mayewski, P. A., Rohling, E. E., Curt Stager, J., Karlén, W., Maasch, K. A., David Meeker, L., Meyerson, E. A., Gasse, F., van Kreveld, S., Holmgren, K., Lee-Thorp, J., Rosqvist, G., Rack, F., Staubwasser, M., Schneider, R. R., and Steig, E. J.: Holocene climate variability, Quaternary Res. 62, 243-255, DOI: 10.1016/j.yqres.2004.07.001, 2004.

Mladenov, N., Pulido-Villena, E., Morales-Baquero, R., Ortega-Retuerta, E., Sommaruga, R., and Reche, I.: Spatiotemporal drivers of dissolved organic matter in high alpine lakes: Role of Saharan dust inputs and bacterial activity, J. Geophys. Res.-Biogeo., 113, DOI:10.1029/2008JG000699, 2008.

Mladenov, N., Sommaruga, R., Morales-Baquero, R., Laurion, I., Camarero, L., Diéguez,M. C., Camacho, A., Delgado, A., Torres, O., Chen, Z., Felip, M., and Reche, I.: Dust inputs and bacteria influence dissolved organic matter in clear alpine lakes, Nat. Commun. 2, 405, DOI:10.1038/ncomms1411, 2011.

Morales-Baquero, R., Carrillo, P., Reche, I., and Sánchez-Castillo, P.: Nitrogen-phosphorus relationship in high mountain lakes: effects of the size of catchment basins, Can. J. Fish. Aquat. Sci., 56, 1809-1817, DOI:10.1139/cjfas-56-10-1809, 1999.

Morales-Baquero, R., Pulido-Villena, E., and Reche, I.: Atmospheric inputs of phosphorus and nitrogen to the southwest Mediterranean region: Biogeochemical responses of high mountain lakes, Limnol. Oceanogr., 51, 830-837, DOI:10.4319/lo.2006.51.2.0830, 2006a.

Morales-Baquero R., Pulido-Villena, E., Romera, O., Ortega-Retuerta, E., Conde-Porcuna, J. M., Pérez-Martinez, C., and Reche, I.: Significance of atmospheric deposition to freswater ecosystems in the southern Iberian Peninsula, Limnetica, 25, 171-180, 2006b.

Morales-Baquero, R., Pulido-Villena, E., and Reche, I.: Chemical signature of Saharan dust on dry and wet atmospheric deposition in the south-western Mediterranean region, Tellus B, 65, DOI:10.3402/tellusb.v65i0.18720, 2013.

Morales-Baquero, R., and Pérez-Martínez C.: Saharan versus local influence on atmospheric aerosol deposition in the southern Iberian Peninsula: Significance for N and P inputs, Global Biogeochem. Cycles, 30, 501-513,DOI:10.1002/2015GB005254, 2016.

Moreno, A., Pérez, A., Frigola, J., Nieto-Moreno, V., Rodrigo-Gámiz, M., Martrat, B., González-Sampériz, P., Morellón, M., Martín-Puertas, C., Corella, J. P., Belmonte, A., Sancho, C., Cacho, I., Herrera, G., Canals, M., Grimalt, J. O., Jiménez-Espejo, F. J., Martínez-Ruiz, F., Vegas-Villarrúbia, T., and Valero-Garcés, B. L.: The Medieval Climate Anomaly in the Iberian Peninsula reconstructed from marine and lake records, Quaternary Sci. Rev., 42, 16-32, DOI:10.1016/j.quascirev.2012.04.007, 2012.

Moreno, T., Querol, X., Castillo, S., Alastuey, A., Cuevas, E., Herrmann, L., Mounkaila, M., Elvira, J., Gibbons, W.: Geochemical variations in aeolian mineral particles from the Sahara–Sahel Dust Corridor. Chemosphere, 65, 261-270, DOI:10.1016/j.chemosphere.2006.02.052, 2006.

Morellón, M., Valero-Garcés, B., Vegas-Vilarrúbia, T., González-Sampériz, P., Romero, O., Delgado-Huertas, A., Mata, P., Moreno, A., Rico, M., and Corella, J. P.: Lateglacial and Holocene palaeohydrology in the western Mediterranean region: the Lake Estanya record (NE Spain), Quaternary Sci. Rev., 28, 2582-2599, DOI:10.1016/j.quascirev.2009.05.014, 2009.

Morellón, M., Valero-Garcés, B., González-Sampériz, P., Vegas-Vilarrúbia, T., Rubio, E., Rieradevall, M., Delgado-Huertas, A., Mata, P., Romero, O., Engstrom, D. R., López-Vicente, M., Navas, A., and Soto, J.: Climate changes and human activities recorded in the sediments of Lake Estanya (NE Spain) during the Medieval Warm Period and Little Ice Age, J. Paleolimnol., 46, 423-452, DOI:10.1007/s10933-009-9346-3, 2011.

Morellón, M., Pérez-Sanz, A., Corella, J. P., Büntgen, U., Catalán, J., González-Samprizé, P., González-Trueba, J. J., López-Sáez, J. A., Moreno, A., Pla, S.,Saz-Sánchez, M. Á., Scussolini, P., Serrano, E., Steinhilber, F., Stefanova, V., Vegas-Vilarrúbia, T., and Saz-Sánchez, M. A.: A multi-proxy perspective on millennium-long climate variability in the Southern Pyrenees, Clim. Past, DOI:10.5194/cpd-7-3049-2011, 2012.

Mulitza, S., Heslop, D., Pittauerova, D., Fischer, H. W., Meyer, I., Stuut, J.-B., Zabel, M., Mollenhauer, G., Collins, J.A., Kuhnert, H., and Schulz, M.: Increase in African dust flux at the onset of commercial agriculture in the Sahel region, Nature, 466, 226-228, DOI:10.1038/nature09213, 2010.

Sobrino, C. M., García-Moreiras, I., Castro, Y., Carreño, N. M., de Blas, E., Rodríguez, C. F., Judd, A., and García-Gil, S., Climate and anthropogenic factors influencing an estuarine ecosystem from NW Iberia: new high resolution multiproxy analyses from San Simón Bay (Ría de Vigo), Quaternary Sci. Rev., 93, 11-33, DOI:10.1016/j.quascirev.2014.03.021, 2014.

Nieto-Moreno, V., Martínez-Ruiz, F., Giralt, S., Jiménez-Espejo, F. J., Gallego-Torres, D., Rodrigo-Gámiz, M., García-Orellana, J., Ortega-Huertas, M., and de Lange, G. J.: Tracking climate variability in the western Mediterranean during the Late Holocene: a multiproxy approach, Clim. Past, 7, 1395-1414, DOI:10.5194/cp-7-1395-2011, 2011.

Nieto-Moreno, V., Martínez-Ruiz, F., Willmott, V., García-Orellana, J., Masqué, P., and Damsté, J. S.: Climate conditions in the westernmost Mediterranean over the last two millennia: An integrated biomarker approach, Org. Geochem., 55, 1-10. DOI:10.1177/0959683613484613, 2013

Nieto-Moreno, V., Martínez-Ruiz, F., Gallego-Torres, D., Giralt, S., García-Orellana, J., Masqué, P., Sinninghe Damsté, J. S., and Ortega-Huertas, M.: Palaeoclimate and palaeoceanographic conditions in the westernmost Mediterranean over the last millennium: an integrated organic and inorganic approach, J. Geol. Soc. London , 172, 264-271, DOI: 10.1144/jgs2013-105, 2015.

Oliva, M., Ruiz-Fernández, J., Barriendos, M., Benito, G., Cuadrat, J. M., Domínguez-Castro, F., García-Ruiz, J. M., Giralt, S., Gómez-Ortiz, A., Hernández, A., López-Costas, O., López-Moreno, J. I., López-Sáez, J. A., Matínez-Cortízar, A., Moreno, A., Prohom, M., Saz, M. A. Serrano, E., Tejedor, E., Trigo, R., Valero-Garcés, B. and López-Costas, O.: The Little Ice Age in Iberian mountains, Earth-Sci. Rev., 177, 175-208, DOI:10.1016/j.earscirev.2017.11.010, 2018.

Olsen, J., Anderson, N. J., and Knudsen, M. F.: Variability of the North Atlantic Oscillation over the past 5,200 years, Nat. Geosci., 5, 808-812, DOI:10.1038/ngeo1589, 2012.

Palma, P., Oliva, M., García-Hernández, C., Ortiz, A. G., Ruiz-Fernández, J., Salvador-Franch, F., and Catarineu, M: Spatial characterization of glacial and periglacial landforms in the highlands of Sierra Nevada (Spain), Sci. Total Environ., 584, 1256-1267, DOI:10.1016/j.scitotenv.2017.01.196, 2017.

Poska, A., and Pidek, I. A.: Pollen dispersal and deposition characteristics of *Abies alba*, *Fagus sylvatica* and *Pinus sylvestris*, Roztocze region (SE Poland). Veg. Hist. Archaeobot., 19, 91-101, DOI:10.1007/s00334-009-0230-x, 2010.

Pulido-Villena, E., Reche, I., and Morales-Baquero, R.: Significance of atmospheric inputs of calcium over the southwestern Mediterranean region: High mountain lakes as tools for detection, Global Biogeochem. Cy., 20, GB2012, DOI:10.1029/2005GB002662, 2006.

Pulido-Villena, E., Wagener, T., and Guieu, C.: Bacterial response to dust pulses in the western Mediterranean: Implications for carbon cycling in the oligotrophic ocean, Global Biogeochem. Cy., 22, DOI:10.1029/2007GB003091, 2008a.

Pulido-Villena, E., Reche, I., and Morales-Baquero, R.: Evidence of an atmospheric forcing on bacterioplankton and phytoplankton dynamics in a high mountain lake, Aquat. sci., 70, 1-9, DOI:10.1007/s00027-007-0944-8, 2008b.

Ramos-Román, M. J., Jiménez-Moreno, G., Anderson, R. S., García-Alix, A., Toney, J. L., Jiménez-Espejo, F. J., and Carrión, J. S.: Centennial-scale vegetation and North Atlantic Oscillation changes during the Late

Holocene in the southern Iberia, Quaternary Sci. Rev., 143, 84-95, DOI:10.1016/j.quascirev.2016.05.007, 2016.

Ramos-Román, M. J.: Holocene paleoenvironmental change, climate and human impact in Sierra Nevada, Southern Iberian Peninsula, Ph. D. Thesis, Universidad de Granada, Granada, 2018.

Ramos-Román, M. J., Jiménez-Moreno, G., Camuera, J., García-Alix, A., Anderson, R. S., Jiménez-Espejo, F. J., Sasche, D., Toney, J. L., Carrión, J. S., Webster, C and Yanes, Y.: Millennial-scale cyclical environment and climate variability during the Holocene in the western Mediterranean region deduced from a new multi-proxy analysis from the Padul record (Sierra Nevada, Spain), Glob. Planet. Change, 168, 35-53, DOI:10.1016/j.gloplacha.2018.06.003, 2018a.

Ramos-Román, M. J., Jiménez-Moreno, G., Camuera, J., García-Alix, A., Anderson, R. S., Jiménez-Espejo, F. J., and Carrión, J. S.: Holocene climate aridification trend and human impact interrupted by millennial- and centennial-scale climate fluctuations from a new sedimentary record from Padul (Sierra Nevada, southern Iberian Peninsula), Clim. Past, 14, 117-137, DOI:10.5194/cp-14-117-2018, 2018b.

Rasmussen, S. O., Vinther, B. M., Clausen, H. B., and Andersen, K. K.: Early Holocene climate oscillations recorded in three Greenland ice cores, Quaternary Sci. Rev., 26, 1907-1914, DOI:10.1016/j.quascirev.2007.06.015, 2007.

Reche, I., Ortega-Retuerta, E., Romera, O., Villena, E. P., Baquero, R. M., and Casamayor, E. O.: Effect of Saharan dust inputs on bacterial activity and community composition in Mediterranean lakes and reservoirs, Limnol. Oceanogr., 54, 869-879, DOI:10.4319/lo.2009.54.3.0869, 2009.

Reed, J. M., Stevenson, A. C., and Juggins, S.: A multi-proxy record of Holocene climatic change in southwestern Spain: the Laguna de Medina, Cádiz, Holocene, 11, 707-719, DOI:10.1191/09596830195735, 2001.

Reimer, P. J., Bard, E., Bayliss, A., Beck, J. W., Blackwell, P. G., Bronk Ramsey, C., Buck, C. E., Cheng, H., Edwards, R. L., Friedrich, M., Grootes, P. M., Guilderson, T. P., Haflidason, H., Hajdas, I., Hatté, C., Heaton, T. J., Hoffmann, D. L., Hogg, A. G., Hughen, K. A., Kaiser, K. F., Kromer, B., Manning, S. W., Niu, M., Reimer, R. W., Richards, D. A., Scott, M., Southon, J. R., Staff, R. A., Turney, C. S. M., and van der Plicht, J.: IntCal13 and Marine13 radiocarbon age calibration curves 0-50,000 years cal BP, Radiocarbon, 55, 1869-1887, DOI:10.2458/azu_js_rc.55.16947, 2013.

Regattieri, E., Zanchetta, G., Drysdale, R. N., Isola, I., Hellstrom, J. C., Dallai, L.: Lateglacial to holocene trace element record (Ba, Mg, Sr) from Corchia cave (Apuan Alps, central Italy): paleoenvironmental implications, J. Quat. Sci., 29, 381-392, DOI:10.1002/jqs.2712, 2014.

Révillon, S., Jouet, G., Bayon, G., Rabineau, M., Dennielou, B., Hémond, C., and Berné, S.: The provenance of sediments in the Gulf of Lions, western Mediterranean Sea, Geochem. Geophy. Geosy., 12, Q08006, DOI:10.1029/2011GC003523, 2011.

Rodrigo-Gámiz, M., Martínez-Ruiz, F., Jiménez-Espejo, F. J., Gallego-Torres, D., Nieto-Moreno, V., Romero, O., Ariztegui, D.: Impact of climate variability in the western Mediterranean during the last 20,000 years: oceanic and atmospheric responses, Quaternary Sci. Rev., 30, 2018-2034, DOI:10.1016/j.quascirev.2011.05.011, 2011.

Sawatzky, C. L., Wurtsbaugh, W. A., Luecke, C.: The spatial and temporal dynamics of deep chlorophyll layers in high-mountain lakes: effects of nutrients, grazing, and herbivore recycling as growth determinants, J. Plankton Res., 28, 65–86, DOI:10.1093/plankt/fbi101, 2006.

Schulte, L.: Climatic and human influence on river systems and glacier fluctuations in southeast Spain since the Last Glacial Maximum, Quatern. Int., 93-94, 85-100, DOI:10.1016/S1040-6182(02)00008-3, 2002.

Sánchez-López, G., Hernández, A., Pla-Rabes, S., Trigo, R. M., Toro, M., Granados, I., Sáez, A., Masqué, P., Pueyo, J. J., Rubio-Inglés, M. J., and Giralt, S.: Climate reconstruction for the last two millennia in central Iberia: The role of East Atlantic (EA), North Atlantic Oscillation (NAO) and their interplay over the Iberian Peninsula, Quaternary Sci. Rev., 149, 135-150, DOI:10.1016/j.quascirev.2016.07.021, 2016.

Settle D. M., and Patterson C. C.: Lead in Albacore: guide to lead pollution in Americans, Science, 207, 1167-76, DOI:10.1126/science.6986654 ,1980.

Solanki, S. K., Usoskin, I. G., Kromer, B., Schüssler, M., and Beer, J.: Unusual activity of the Sun during recent decades compared to the previous 11,000 years, Nature, 431, 1084-1087, DOI:10.1038/nature02995, 2004.

Tjallingii, R., Röhl, U., Kölling, M., and Bickert, T.: Influence of the water content on X-ray fluorescence core-scanning measurements in soft marine sediments, Geoch. Geophy. Geosy., 8, DOI:10.1029/2006GC001393, 2007.

Trigo, R. M., and Palutikof, J. P.: Precipitation scenarios over Iberia: a comparison between direct GCM output and different downscaling techniques, J. Climate , 14, 4442-4446, DOI:10.1175/1520-0442(2001)014<4422:PSOIAC>2.0.CO;2, 2001.

Trigo, R. M., Pozo-Vázquez, D., Osborn, T. J., Castro-Díez, Y., Gámiz-Fortis, S., and Esteban-Parra, M. J.: North Atlantic Oscillation influence on precipitation, river flow and water resources in the Iberian Peninsula, Int. J. Climatol., 24, 925-944, DOI:10.1002/joc.1048, 2004.

Trouet, V., Esper, J., Graham, N. E., Baker, A., Scourse, J. D., and Frank, D. C.: Persistent positive North Atlantic Oscillation mode dominated the Medieval Climate Anomaly, Science, 324, 78-80, DOI:10.1126/science.1166349, 2009.

Valbuena-Carabaña, M., López de Heredia, U., Fuentes-Utrilla, P., González-Doncel, I., and Gil, L.: Historical and recent changes in the Spanish forests: a socioeconomic process, Rev. Palaeobot. Palyno., 162, 492-506, DOI:10.1016/j.revpalbo.2009.11.003, 2010.

Valle, F.: Mapa de series de vegetación de Andalucía 1: 400 000, Editorial Rueda, Madrid, 2003.

Van der Weijden, C. H.: Pitfalls of normalization of marine geochemical data using a common divisor, Mar. Geol., 184, 167-187, DOI:10.1016/S0025-3227(01)00297-3, 2002.

Walczak, I. W., Baldini, J. U., Baldini, L. M., McDermott, F., Marsden, S., Standish, C. D., Richards, D. A., Andreo, B., and Slater, J.: Reconstructing high-resolution climate using CT scanning of unsectioned stalagmites: A case study identifying the mid-Holocene onset of the Mediterranean climate in southern Iberia, Quaternary Sci. Revi., 127, 117-128, DOI:10.1016/j.quascirev.2015.06.013, 2015.

Wanner, H., Brönnimann, S., Casty, C., Gyalistras, D., Luterbacher, J., Schmutz, C., Stephenson, D. B., and Xoplaki, E.: North Atlantic Oscillation–concepts and studies, Surv. Geophys., 22, 321-381, DOI:10.1023/A:1014217317898, 2001.

Wiersma, A. P., and Jongma, J. I.: A role for icebergs in the 8.2 ka climate event, Climate dynamics, 35, 535-549, DOI:10.1007/s00382-009-0645-1, 2010.

Wiersma, A. P., Roche, D. M., and Renssen, H.: Fingerprinting the 8.2 ka event climate response in a coupled climate model, J. Quat. Sci., 26, 118-127, DOI:10.1002/jqs.1439, 2011.

Yuan, F.: A multi-element sediment record of hydrological and environmental changes from Lake Erie since 1800, J. Paleolimnol., 58, 23-42, DOI:10.1007/s10933-017-9953-3, 2017.

Zanchetta, G., Drysdale, R. N., Hellstrom, J. C., Fallick, A. E., Isola, I., Gagan, M. K., Pareschi, M. T.: Enhanced rainfall in the Western Mediterranean during deposition of sapropel S1: stalagmite evidence from Corchia cave (Central Italy), Quaternary Sci. Rev., 26, 279-286, DOI:10.1016/j.quascirev.2006.12.003, 2007.

List of tables

Lab Number	*Depth (cm)*	*Dating Method*	*Age (14C yr BP±1σ)*	*Calibrated age (cal yr BP)2σ ranges*
	0	Present	2012 CE	-63
Poz-72421	7	14C	40±40	29-139
D-AMS 008539	22	14C	1112±32	935-1078
D-AMS 008540	39	14C	2675±30	2750-2809
BETA-411994	44	14C	3350±30	3550-3643
BETA-411995	55.5	14C	5480±30	6261-6318
Poz-72423	57.5	14C	5510±50	6266-6405
Poz-72424	62	14C	6450±50	7272-7433
Poz-72425	74	14C	8620±70	9479-9778

Table 1. Age data for LH 12-03. All ages were calibrated using IntCal13 curve (Reimer et al., 2013) with Clam program (Blaauw, 2010; version 2.2).

	Simulation							
Correlation	A		B		C		D	
Ca/Ca (XRF)	0.63	p<0.01	0.50	p<0.01	0.57	p<0.01	0.54	p<0.01
K/K (XRF)	0.53	p<0.01	0.64	p<0.01	0.56	p<0.01	0.65	p<0.01

Table 2. Simulation of proxy correlation. A) regular interpolation of 300 years sampling spacing. B) regular interpolation of 300 years sampling spacing and 5 data points moving average. C) regular interpolation of 150 years sampling spacing. D) regular interpolation of 150 years sampling spacing and 5 data point moving average.

List of figures

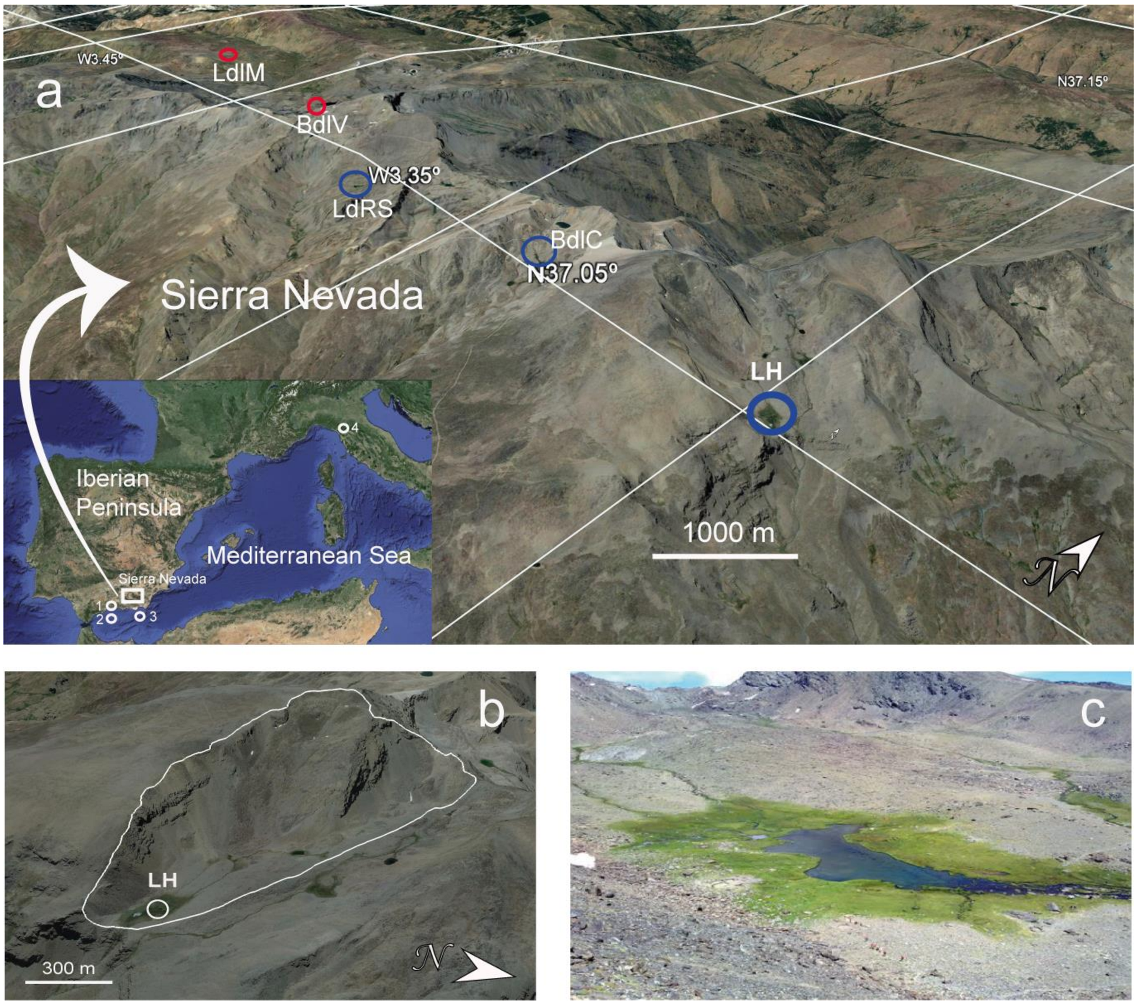

Figure 1. (a) Location of the Laguna Hondera (LH) in Sierra Nevada, southern Iberian Peninsula, along with other nearby records mentioned in the text. (1) El Refugio Cave stalagmite record (Walczak et al., 2015); (2) ODP 976 pollen record (Combourieu-Nebout et al., 2009); (3) MD95-2043 pollen record (Fletcher and Sánchez-Goñi, 2008); (4) CC26, Corchia Cave stalagmite record (Zanchetta et al., 2007; Regattieri et al., 2014). Sierra Nevada north-facing sites are encircled in red, south-facing sites are encircled in blue. LH: Laguna Hondera, the current study, is shown in bold. LdLM: Laguna de la Mula (Jiménez-Moreno et al., 2013); BdLV: Borreguil de la Virgen (García-Alix et al., 2012; Jiménez-Moreno and Anderson, 2012); LdRS: Laguna de Río Seco (Anderson et al., 2011; García-Alix et al., 2013; Jiménez-Espejo et al., 2014); BdlC: Borreguil de la Caldera (Ramos-Román et al., 2016; García-Alix et al., 2017) (b) Regional satellite photo of LH. The white line indicates the catchment area. (c) Photo of Laguna Hondera in September 2012, when the core was taken. Photo taken by Gonzalo Jiménez-Moreno. For the coloured figure, we refer the reader to the web version of this article.

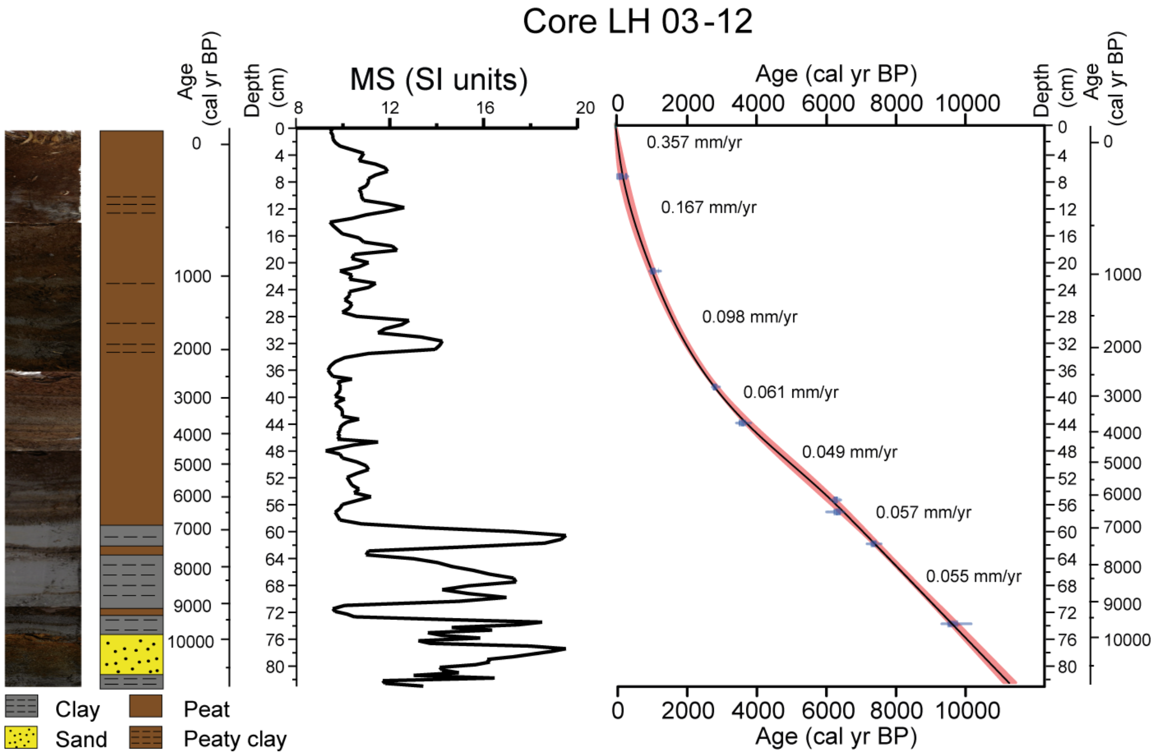

Figure 2. Photo of core LH 12-03, along with the lithology, magnetic susceptibility (MS, in SI units) profile and age-depth model. Sediment accumulation rates (SAR in mm yr $^{-1}$) are shown between individual radiocarbon ages, the red shadow represent the plus/minus range (see details in text for method of construction).

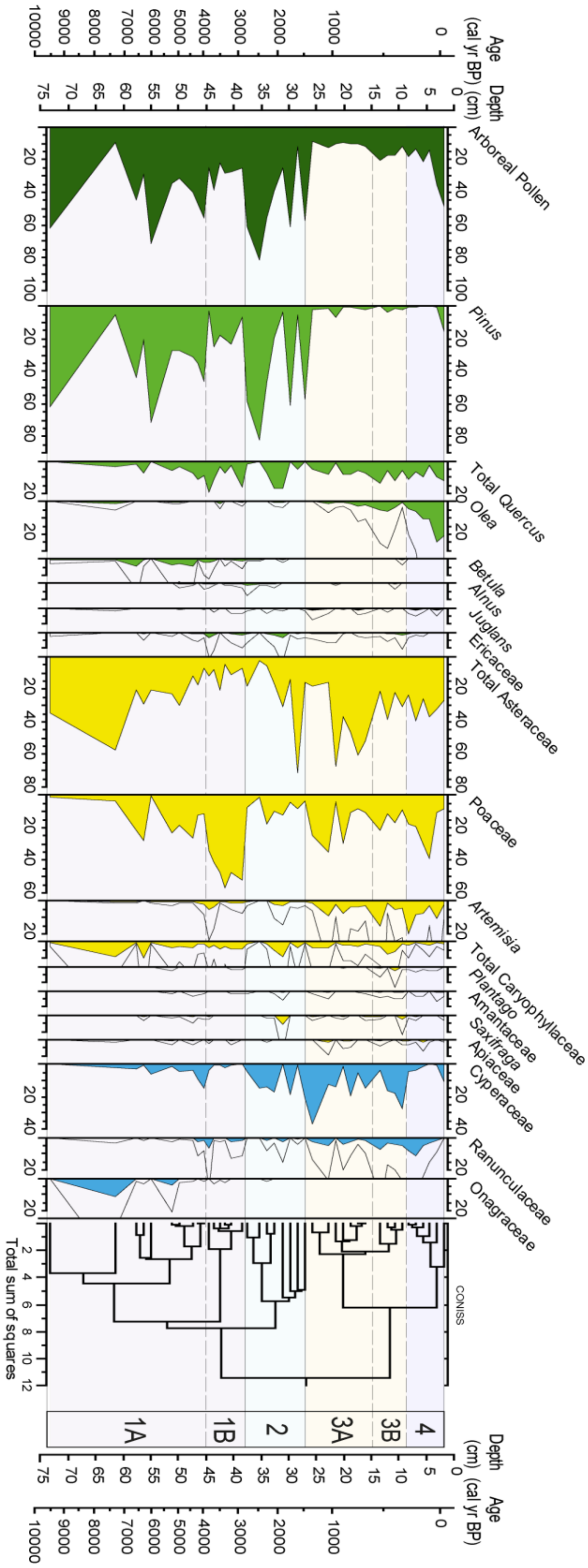

Figure 3. Pollen percentage diagram of the LH 12-03 record showing major selected taxa. Major tree species are shown in green; shrubs and herbs are shown in yellow; and wetland and aquatic types are in blue. Pollen was graphed with the Tilia program (Grimm, 1993), and zoned using the CONISS cluster analysis program (Grimm, 1987).

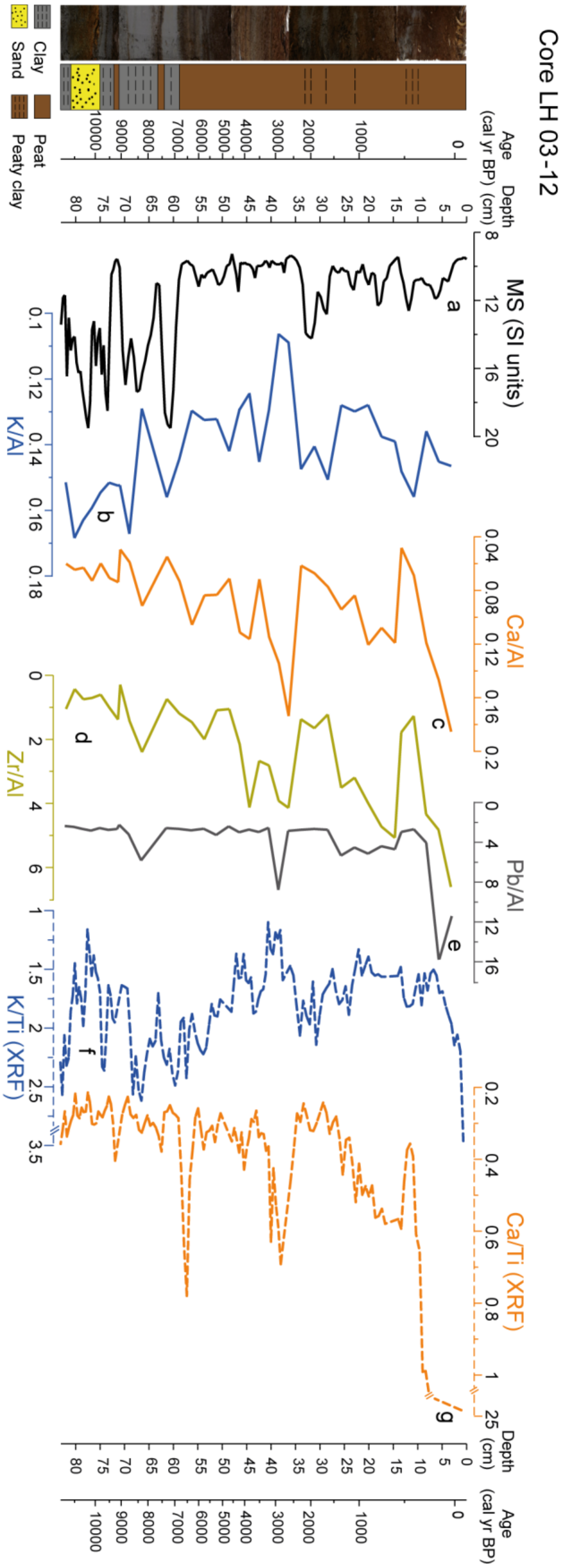

Figure 4. Detailed geochemical diagram of the LH 12-03 record showing the selected proxies: (a) MS; (b) K/Al; (c) Ca/Al; (d) Zr/Al; (e) Pb/Al; (f) K/Ti (XRF); (g) Ca/Ti (XRF) (MS in SI units, Zr/Al and Pb/Al scale x 10^{-4} and XRF in counts).

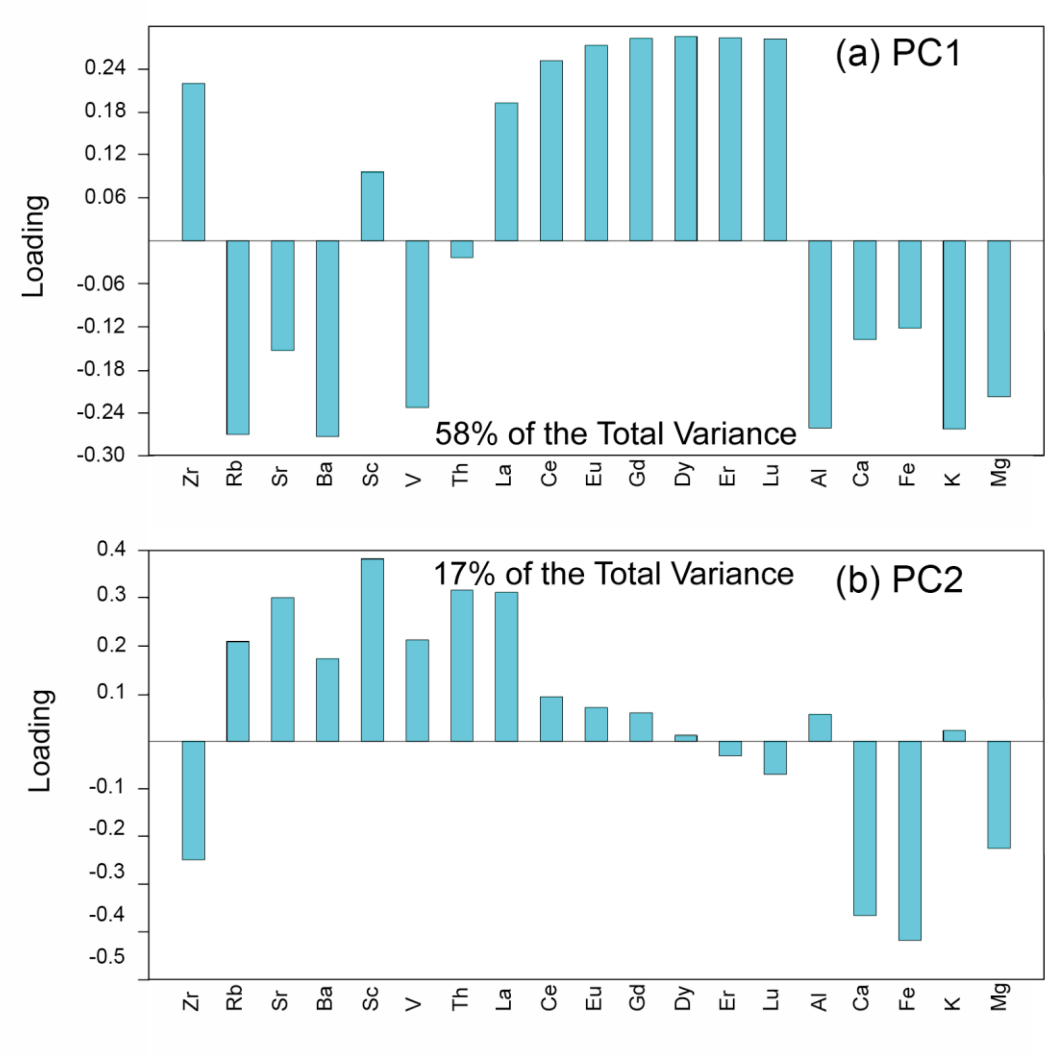

Figure 5. Principal Component Analysis (PCA) loadings from selected geochemical elements. (a) PC1, which describes 58% of total variance; (b) PC2, which describes 17% of total variance.

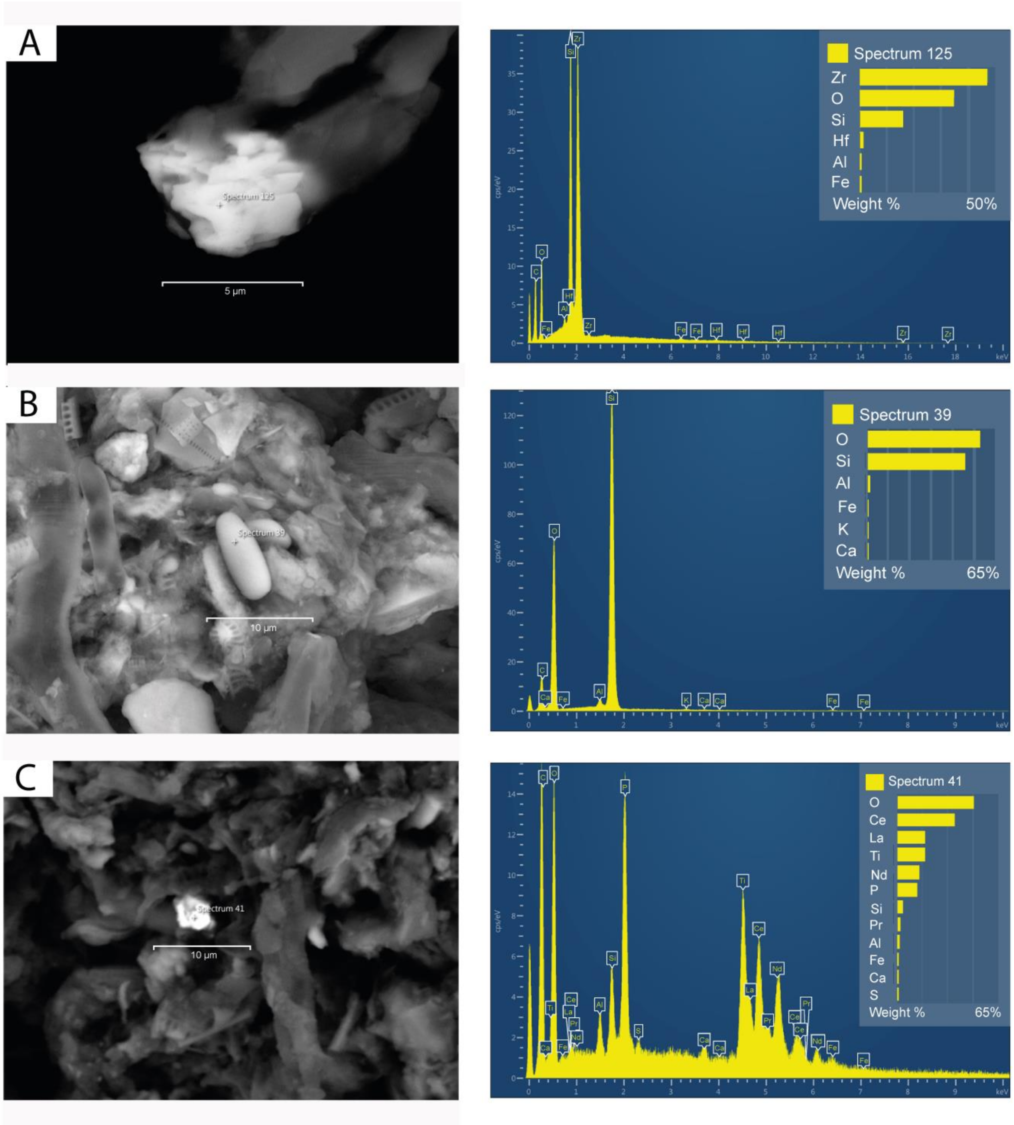

Figure 6. Electron Backscatter Diffraction microphotographs of the Laguna Hondera record with clearer colours representing heavier minerals. The dendrograms represent the elemental composition of each mineral. (a) Zircon, with high Zr content; (b) rounded quartz related with eolian transport; (c) monazite, with high REE content.

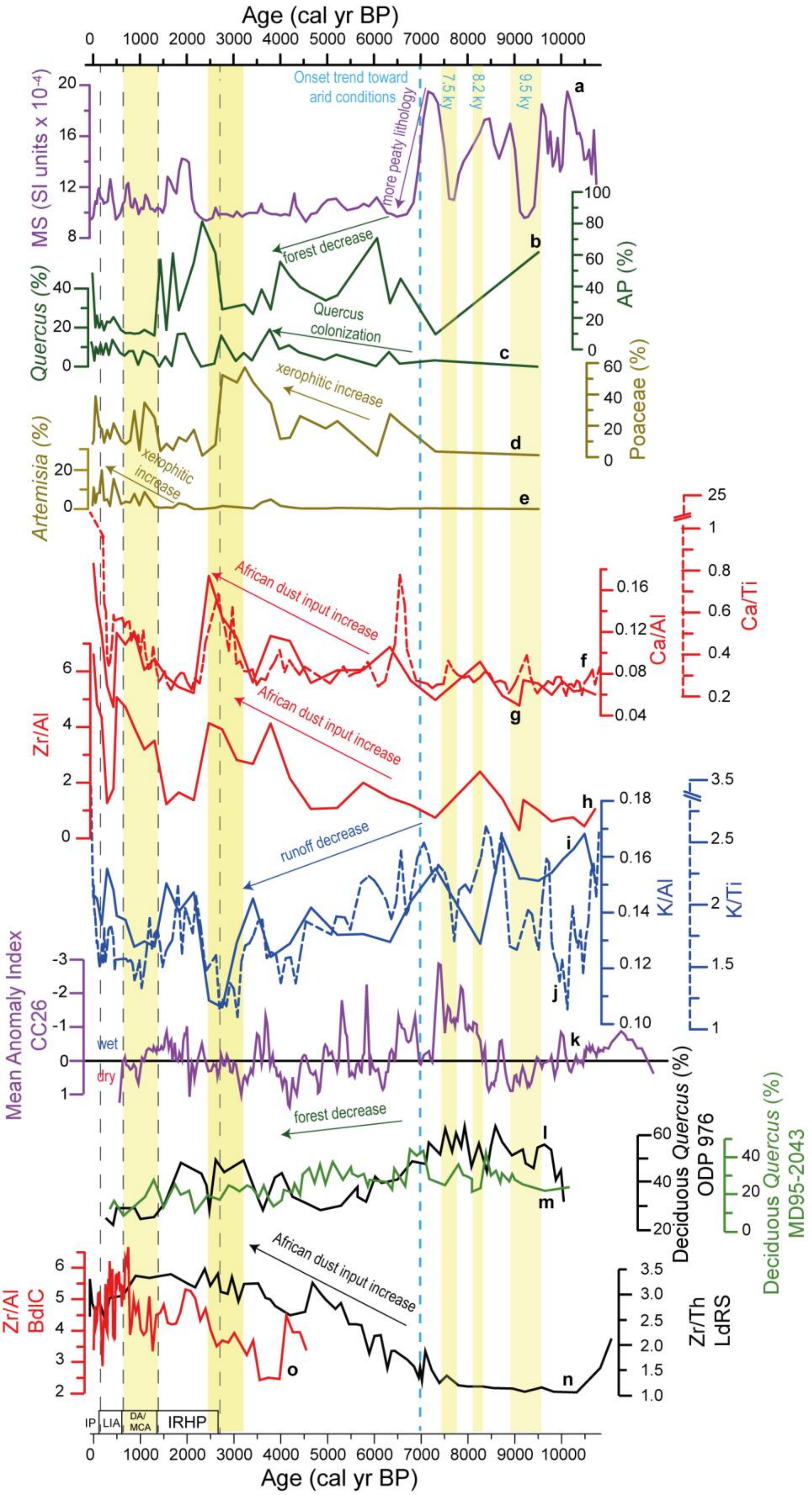

Figure 7. Comparison between the MS data (in SI units x 10^{-4}), the most important pollen taxa and geochemical proxies from Laguna Hondera (LH) record, with nearby paleoclimate records. (a) LH Magnetic Susceptibility (MS) record; (b) Arboreal Pollen (AP) percentage from LH; (c) *Quercus*

percentage from LH; (d) Poaceae percentage from LH; (e) *Artemisia* percentage from LH; (f) Ca/Ti (XRF) ratio from LH in dashed line; (g) Ca/Al ratio from LH; (h) Zr/Al ratio from LH; (i) K/Al ratio from LH; (j) K/Ti (XRF) ratio from LH in dashed line; (k) Mean Anomaly Index from CC26 record (Corchia cave; Regattieri et al., 2014); (l) Deciduous *Quercus* from ODP 976 record (Alboran Sea; Combourieu-Nebout et al., 2009); (m) Deciduous *Quercus* from MD95-2043 record (Alboran Sea; Fletcher and Sanchez-Goñi, 2008); (n) Zr/Th ratio from Laguna de Río Seco (LdRS) (Jiménez-Espejo et al., 2014; García-Alix et al., 2018); (o) Zr/Al ratio from Borreguil de la Caldera (BdlC) (García-Alix et al., 2017; 2018). Yellow bands indicate more arid intervals. Dark dashed lines are used for separating the different Current Era periods: IRHP: Iberian Roman Humid Period; DA: Dark Ages; MCA: Medieval Climate Anomaly; LIA: Little Ice Age; IP: Industrial Period. Blue dashed line indicates the onset of the trend toward arid conditions.

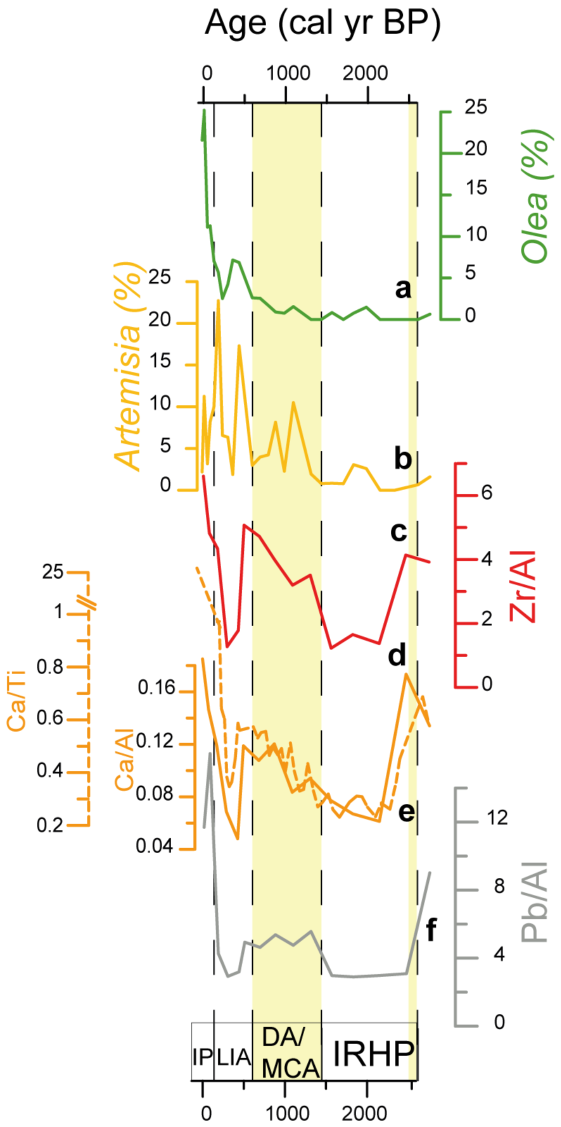

Figure 8. Comparison of geochemical proxies with pollen taxa, related to anthropogenic impact for the last ~2600 cal yr BP. (a) *Olea* percentage from LH; (b) *Artemisia* percentage from LH record; (c) Zr/Al ratio from LH; (d) Ca/Al ratio from LH; (e) Ca/Ti (XRF) ratio from LH in dashed line; (f) Pb/Al ratio from LH. Yellow bands indicate more arid intervals. Dark dashed lines are used for separating the different Current Era periods: IRHP: Iberian Roman Humid Period; DA: Dark Ages; MCA: Medieval Climate Anomaly; LIA: Little Ice Age; IP: Industrial Period.